Neutral pion electro-production in Hall A @ Jefferson Laboratory.

Exclusive 2010

Results released in

arXiv:**1003.2938** [nucl-ex]

submitted to PRC

Eric FUCHEY

Laboratoire de Physique Corpusculaire /

Université Blaise Pascal (Clermont Ferrand)

for the

DVCS/Hall A Collaboration

DVCS experiment E00-110 (2004):

$H(e,e'\gamma)p$ and $H(e,e'\pi^0)p$ events recorded.

DVCS data => [C. Munoz-Camacho *et al*, PRL **97**, 262002 (2006)]

This talk aims to:

- explain how our data were extracted, and convince they are reliable.
- show separated π^0 electro-production cross sections
- emphasize on the difficulty to describe them with the usual models.

Triple coincidence $H(e,e'\gamma\gamma)X$ data

Kinematics

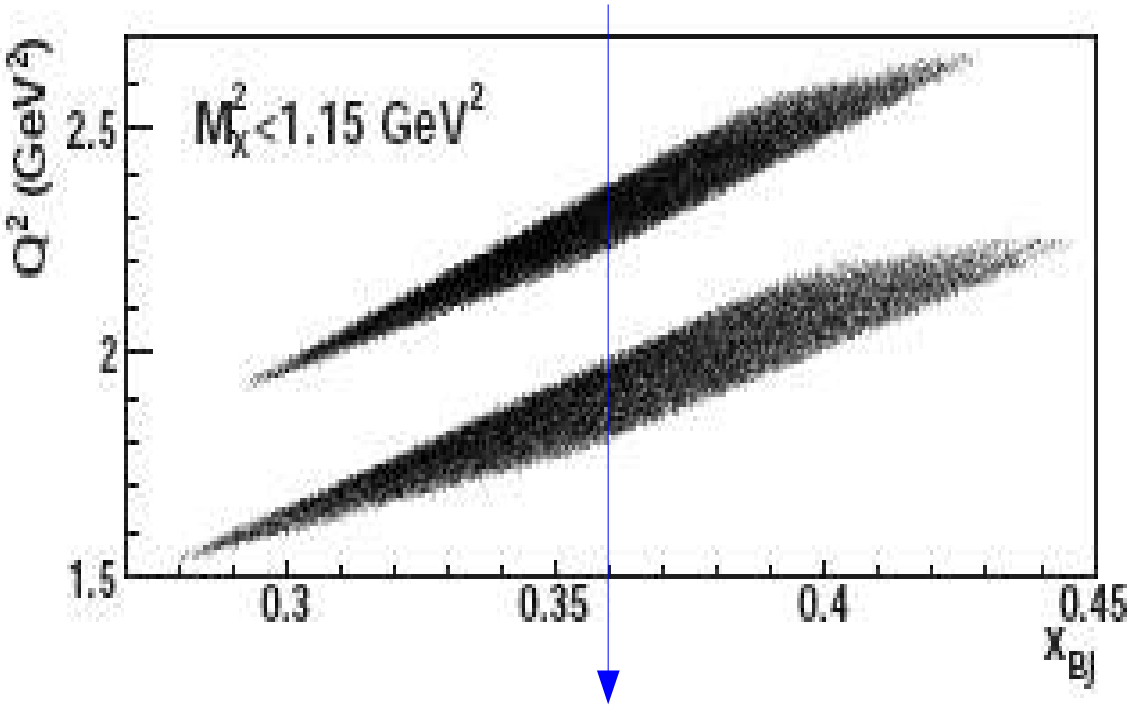

x_{Bj} = 0.36 (Q^2 dependence):

Q^2 = 1.9 GeV^2 (Kin2)

Q^2 = 2.3 GeV^2 (Kin3)

Triple coincidence $H(e,e'\gamma\gamma)X$ data

Kinematics

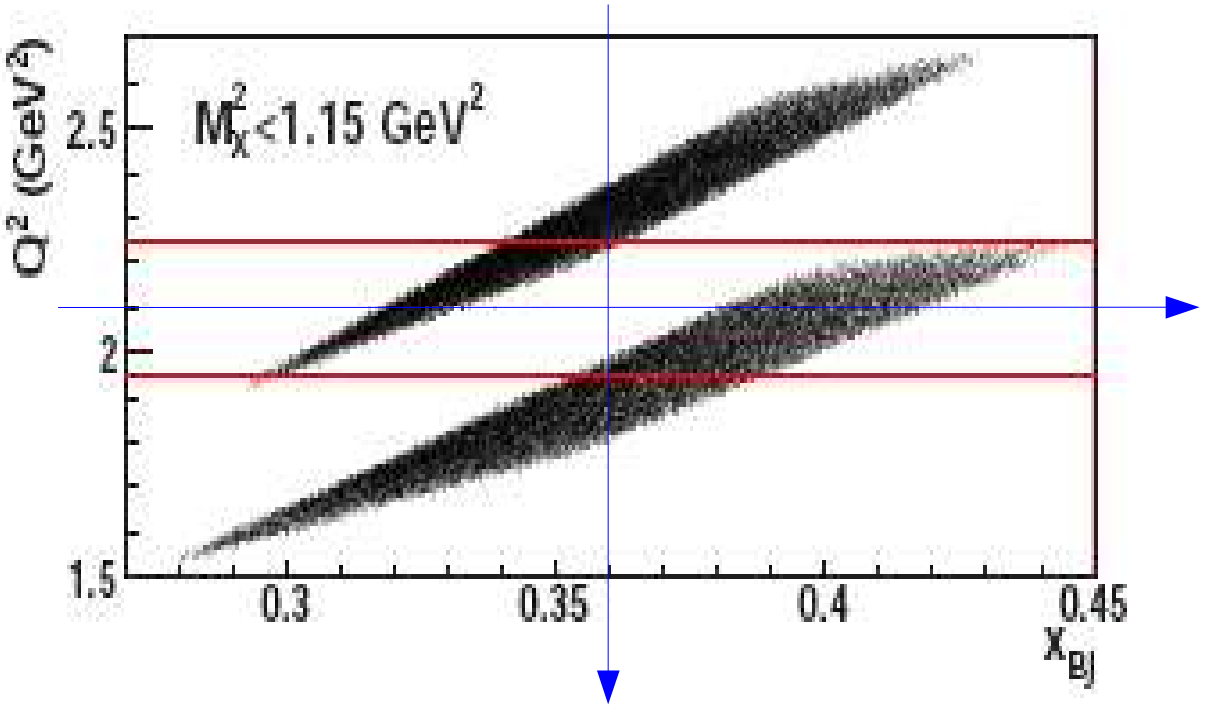

$Q^2 = 2.1$ GeV^2

(W dependence):

$W = 2.0$ GeV (KinX2)

$W = 2.3$ GeV (KinX3)

$x_{Bj} = 0.36$ (Q^2 dependence):

$Q^2 = 1.9$ GeV^2 (Kin2)

$Q^2 = 2.3$ GeV^2 (Kin3)

DVCS (E00-110) apparatus

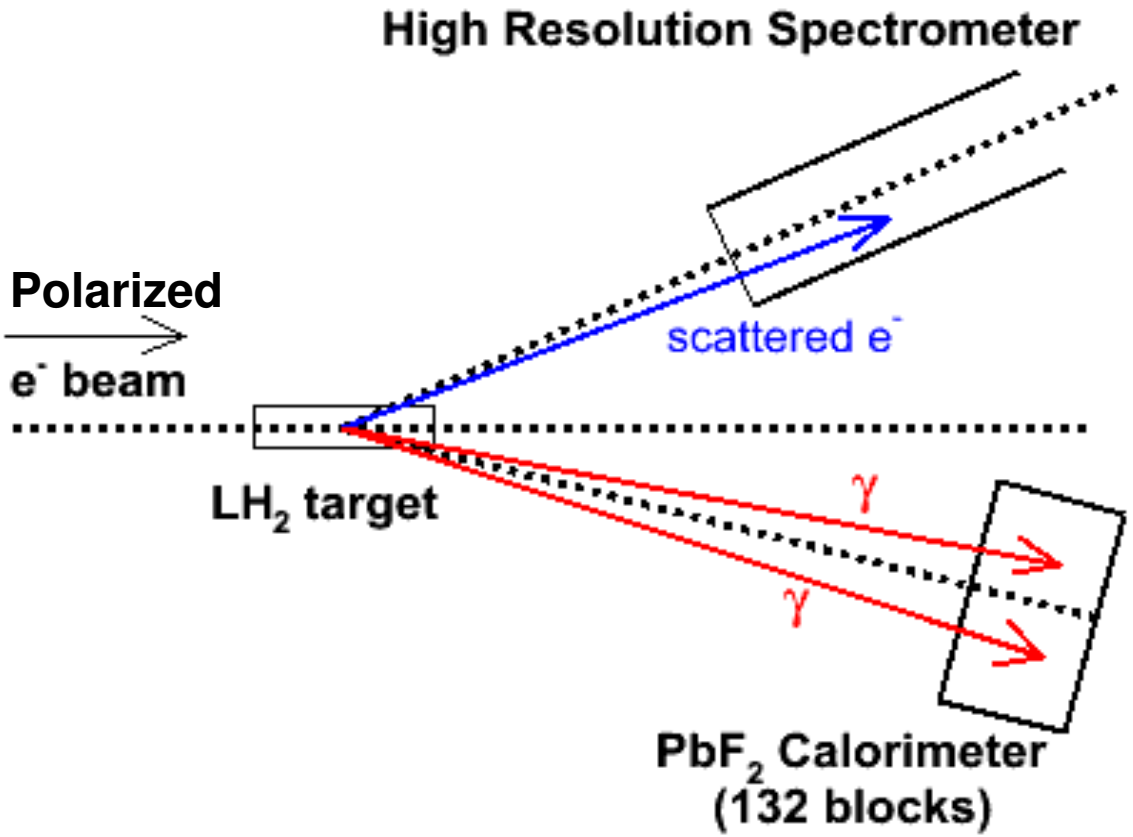

Spectrometer Cuts

$-6.0\ \text{cm} < v < +7.5\ \text{cm}$

$|x_{\text{HRS plan}}| < 3.5\ \text{cm}$

(Horizontal collimator)

$|y_{\text{HRS plan}}| < 7.0\ \text{cm}$

(Vertical collimator)

$|k' - p_{\text{HRS}}|/p_{\text{HRS}} < 4.5\%$

$r > +0.005$

DVCS (E00-110) apparatus

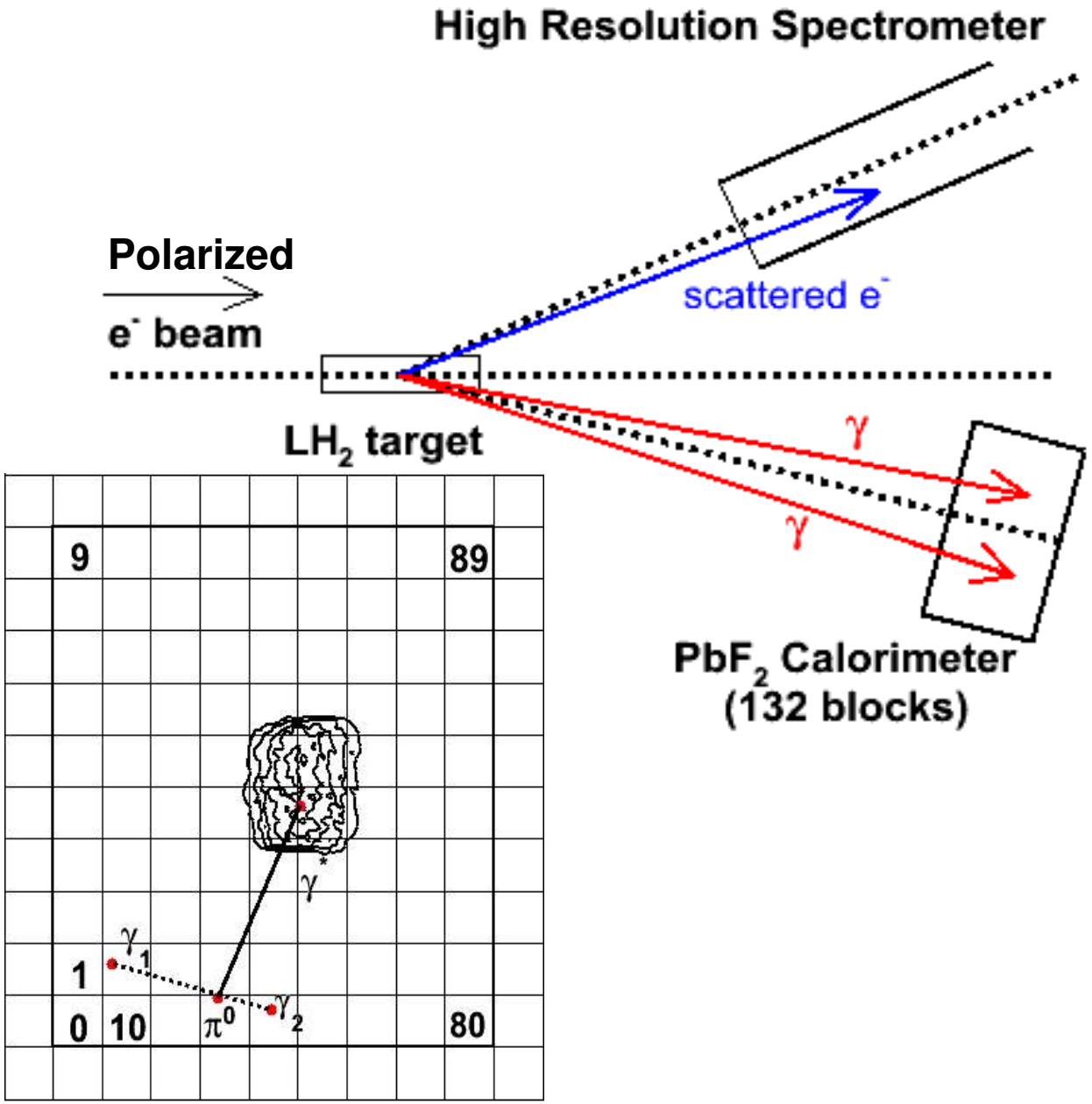

Spectrometer Cuts
$-6.0\ \text{cm} < v < +7.5\ \text{cm}$
$\lvert x_{\text{HRS plan}}\rvert < 3.5\ \text{cm}$
(Horizontal collimator)
$\lvert y_{\text{HRS plan}}\rvert < 7.0\ \text{cm}$
(Vertical collimator)
$\lvert k' - p_{\text{HRS}}\rvert / p_{\text{HRS}} < 4.5\%$
$r > +0.005$
Calorimeter Cuts
$-15.0\ \text{cm} < x_{calo} < +12.0\ \text{cm}$
$\lvert y_{calo}\rvert < 15.0\ \text{cm}$

DVCS (E00-110) apparatus

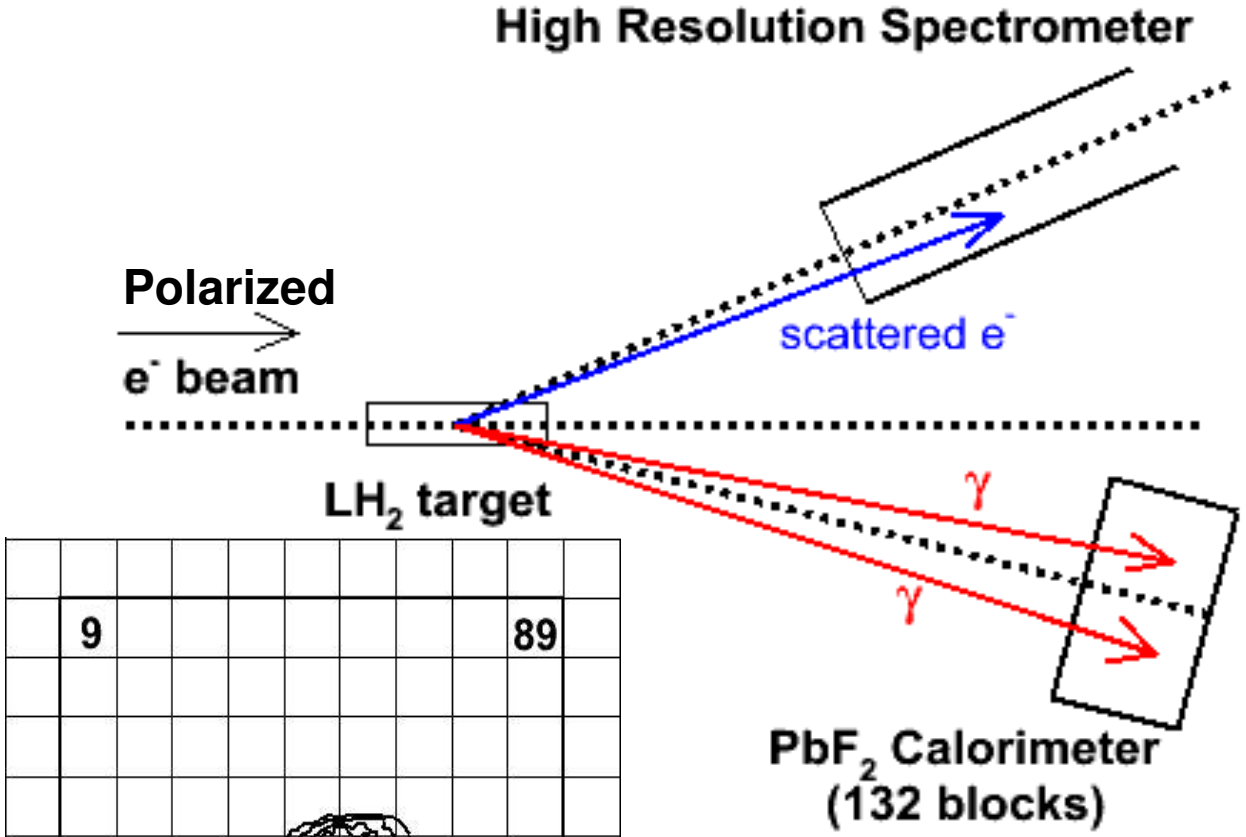

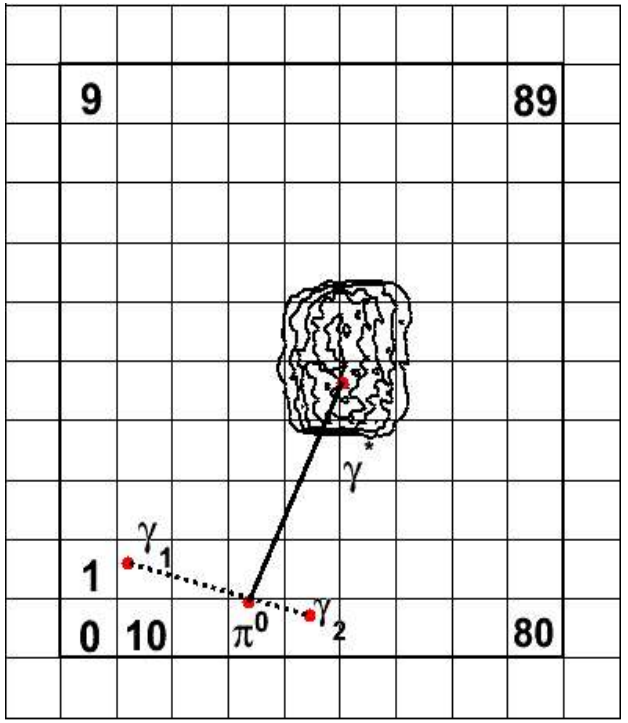

Spectrometer Cuts
$-6.0\ \text{cm} < v < +7.5\ \text{cm}$
$\lvert x_{\text{HRS plan}}\rvert < 3.5\ \text{cm}$
(Horizontal collimator)
$\lvert y_{\text{HRS plan}}\rvert < 7.0\ \text{cm}$
(Vertical collimator)
$\lvert k' - p_{\text{HRS}}\rvert / p_{\text{HRS}} < 4.5\%$
$r > +0.005$
Calorimeter Cuts
$-15.0\ \text{cm} < x_{calo} < +12.0\ \text{cm}$
$\lvert y_{calo}\rvert < 15.0\ \text{cm}$

Exclusive events

-> missing mass $M_X^2 = (k + p - k' - q_1 - q_2)^2$

π^o identification

-> 2γ invariant mass $m_{\gamma\gamma} = \sqrt{(q_1 + q_2)^2}$

Experimental challenge:

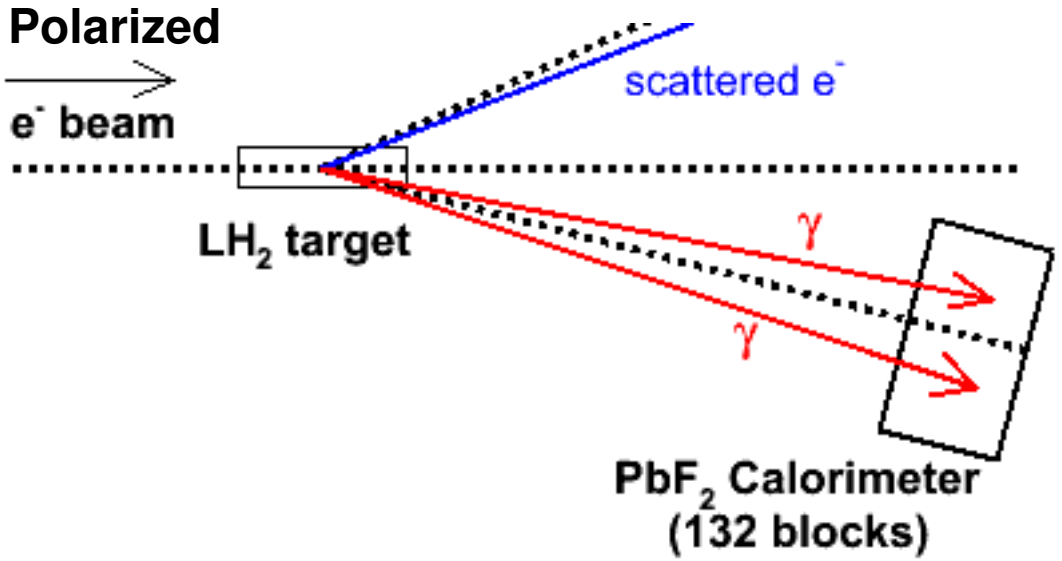

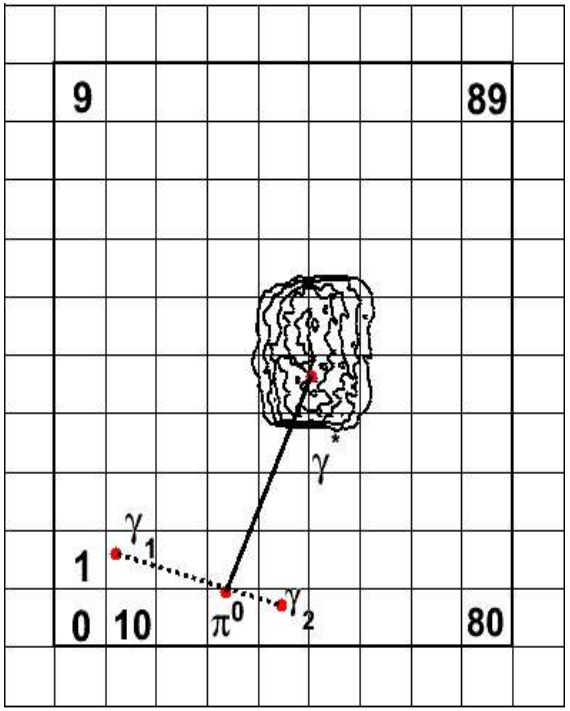

⊙ **Beam**

Experimental challenge:

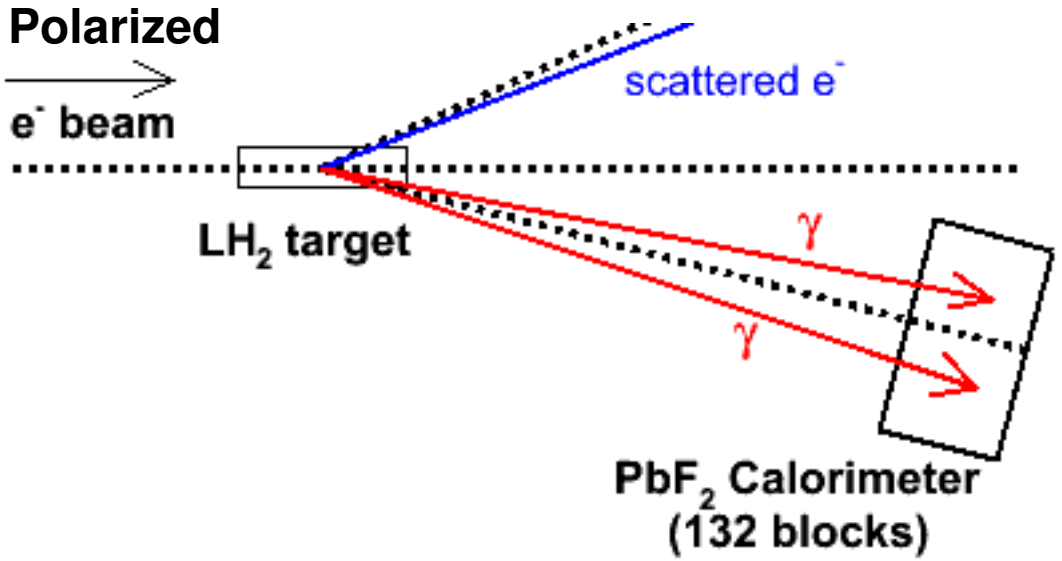

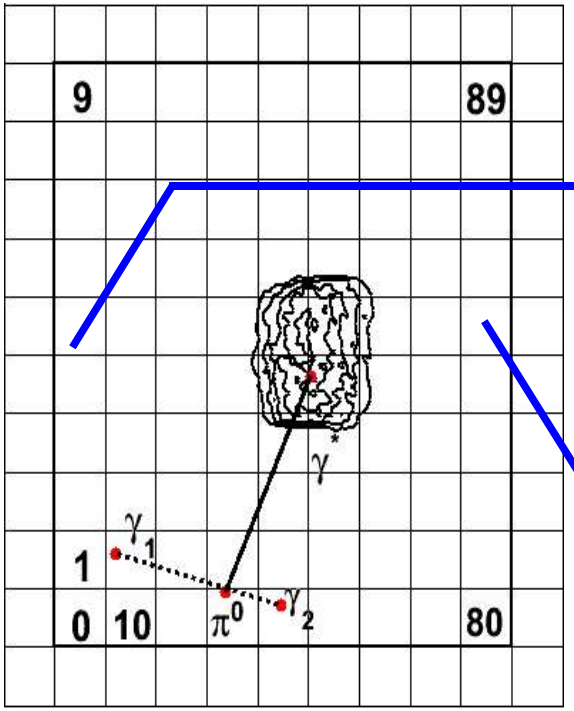

Beam

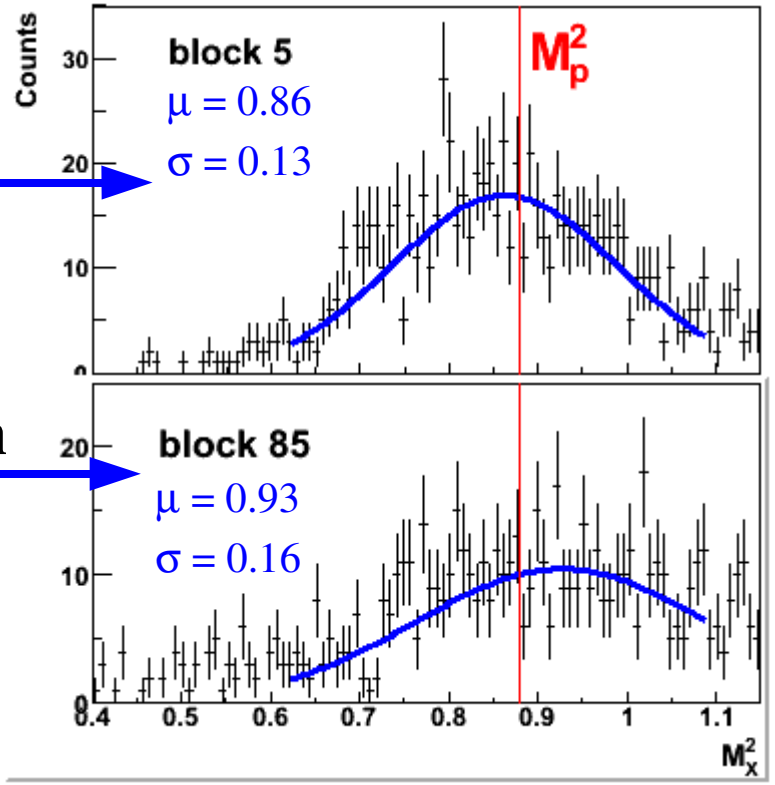

Noise affects position and resolution of missing mass squared, depending on the localization of the block in the calorimeter

=> M_X^2 cut brings spurious $cos\ \phi$ dependence if not corrected (σ_{TL})

=> Calibration

Data: Event-by-event correction of the two photon energies simultaneously to bring each block missing mass squared to M_p^2.

=> calibration coefficients correlated: need to process by iterations.

Simulation: Event-by-event correction + smearing of the two photon energies, to bring the missing mass squared position and resolution of each block for the simulation the same as they are for the data.

Calibration

Data

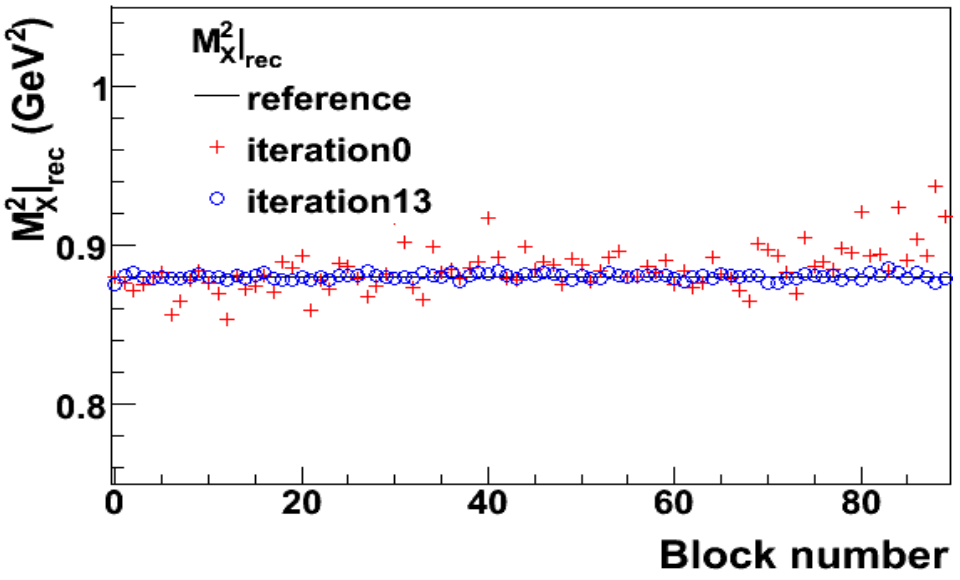

Simulation

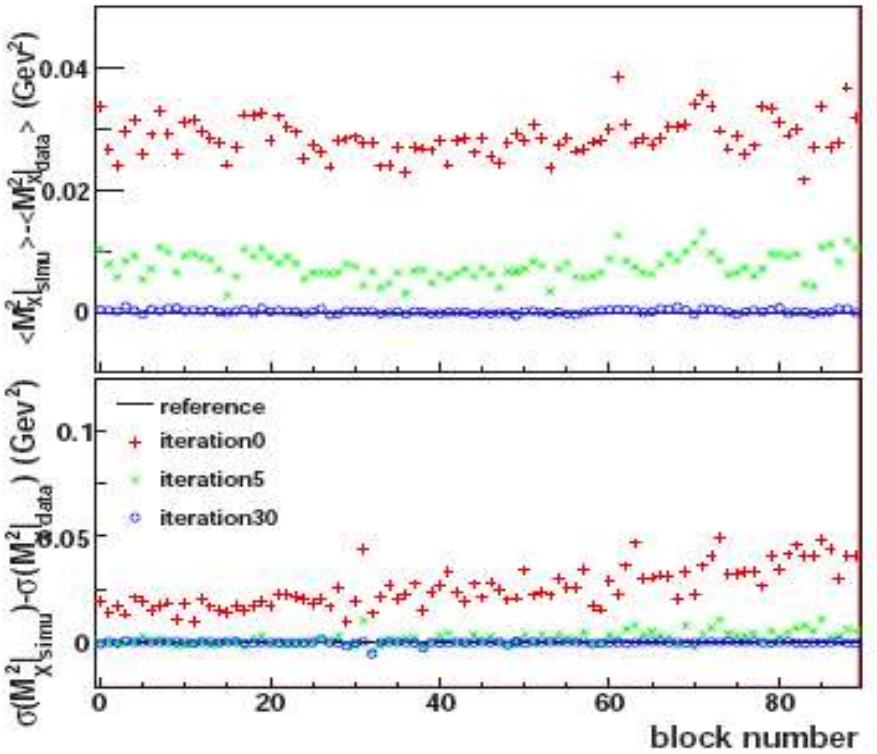

	$\langle m - m_{\pi^0} \rangle$ (GeV)	$\sqrt{\langle (m - m_{\pi^0})^2 \rangle}$ (GeV)
KIN 3		
data	-0.00081	0.0088
simulation	+0.00072	0.0089
KIN 2		
data	-0.00017	0.0079
simulation	+0.00191	0.0085

π^0 mass , resolution

Pion electro-production: Cross section usual formalism

$$\frac{d^5\sigma}{d\Omega_e\, dk'^0\, d\Omega_\pi} = \Gamma \frac{d\sigma_v}{d\Omega_\pi} \qquad \Gamma = \frac{\alpha}{2\pi}\frac{k'^0}{k^0}\frac{k_\gamma}{Q^2}\frac{1}{1-\epsilon}$$

Virtual Photon Flux

$$\left(k_\gamma = \frac{W^2 - M^2}{2M}\right)$$

energy of a real photon giving the same final state

$$\frac{d\sigma_v}{d\Omega_\pi} = \frac{d\sigma_T}{d\Omega_\pi} + \epsilon_L \frac{d\sigma_L}{d\Omega_\pi} + \left[2\,\epsilon_L(1+\epsilon)\right]^{1/2}\frac{d\sigma_{TL}}{d\Omega_\pi}\cos(\phi_\pi) + \epsilon\frac{d\sigma_{TT}}{d\Omega_\pi}\cos(2\,\phi_\pi)$$

$$+ h\left[2\,\epsilon_L(1-\epsilon)\right]^{1/2}\frac{d\sigma_{TL'}}{d\Omega_\pi}\sin(\phi_\pi)$$

ε degree of transverse polarization.

ε_L degree of longitudinal polarization.

extracted in all bins by a linear fit (χ^2 method)

Cross section analysis

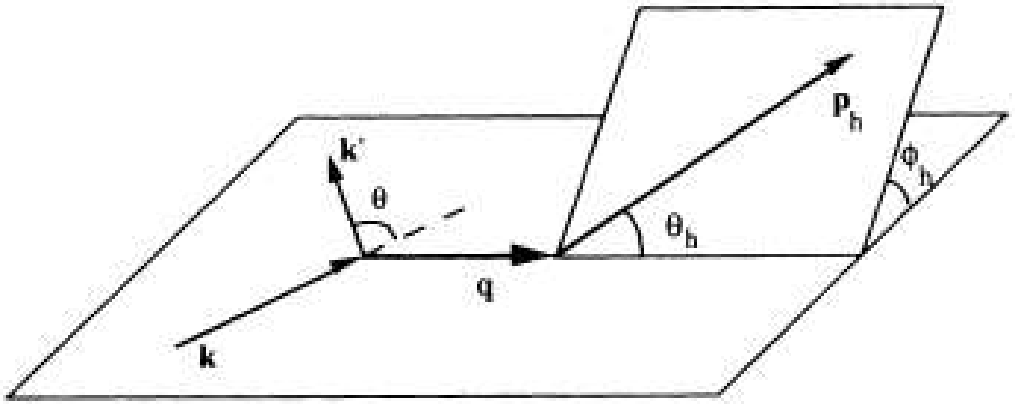

Binning:

24 equal bins in ϕ_π

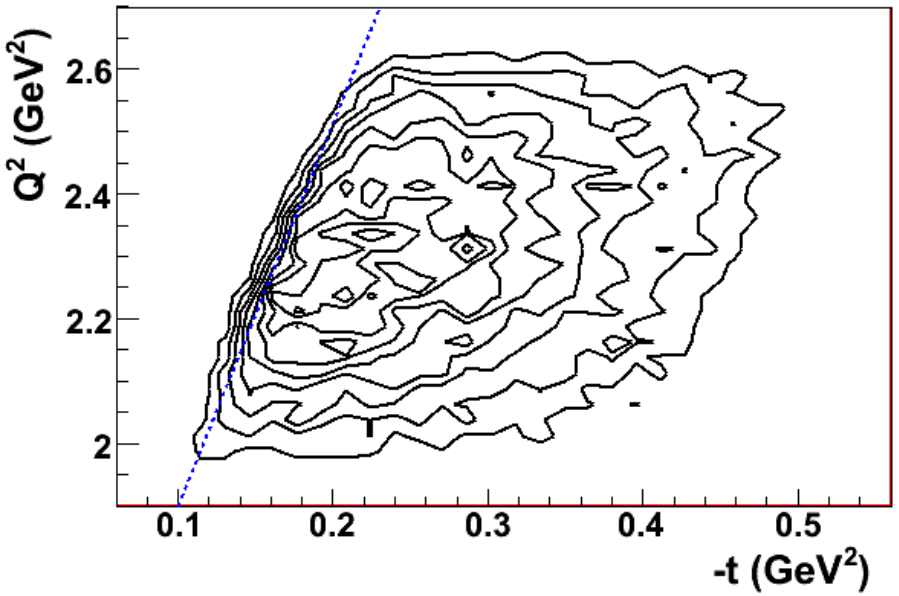

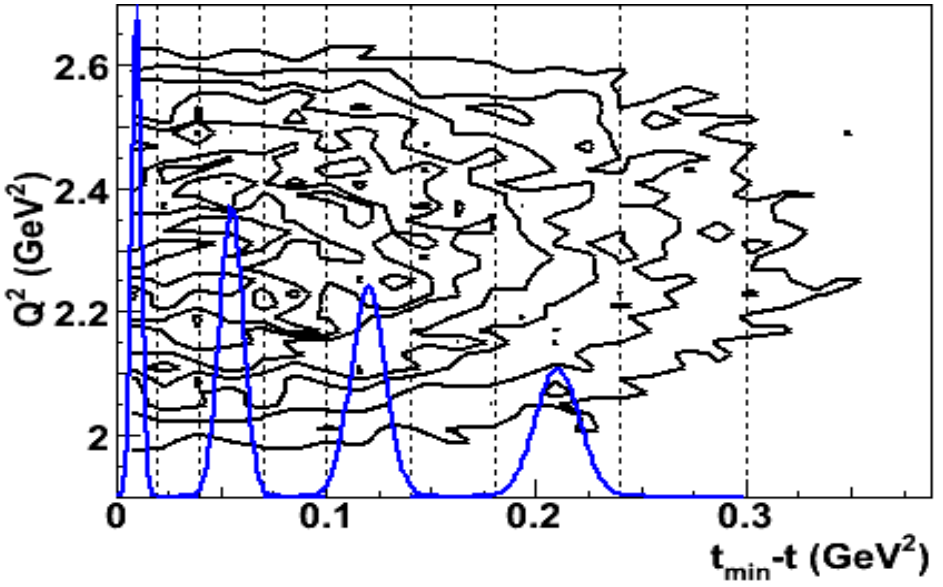

$\theta_\pi^{CM} = f(t)$ variable with Q^2 value.

=> more relevant to analyze in t_{min}-t instead of t (8 bins)

Radiative corrections

Radiative effects:

-> external (Geant simulation)

-> internal real (radiator equivalent approximation in simulation)

-> internal virtual (prescription of M. Vanderhaeghen for DVCS):

=> 0.91 ± 0.02 for all kinematics.

Systematic errors

Cross section depends on M_X^2 cut and $E_{Threshold}$ => have to evaluate the domains where cross section is stable.

Missing mass squared cut:

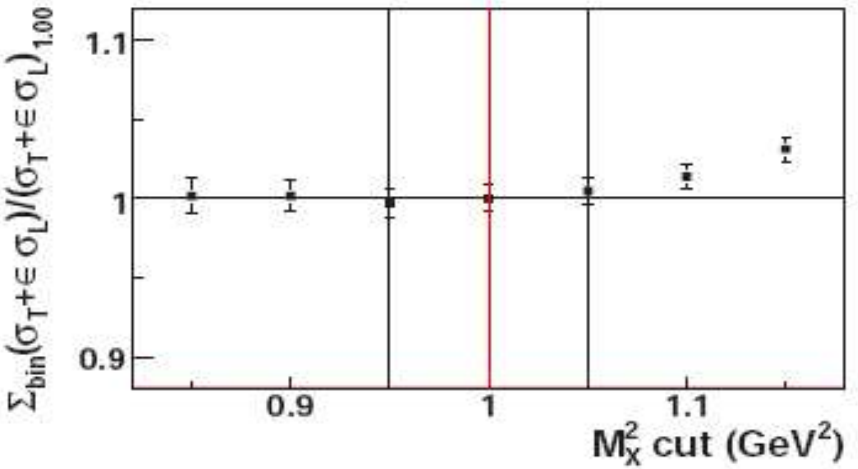

if M_X^2 cut too high: data includes 2,3,... π channels, Δ channels, etc...

if M_X^2 cut too low: removes too much statistics.

Calorimeter threshold...

Other sources of systematic errors

HRS acceptance	2.2 %
Radiative corrections	1.5 %
Target length	0.5 %
Multi tracks corrections	0.1 %
2 clusters corrections	0.1 %
Charge	0.1 %
Dead time	0.1 %
Cerenkov	0.1 %
Total Quadratic	2.7 %
Beam polarization	2.0 %
Total Quadratic	3.37 %

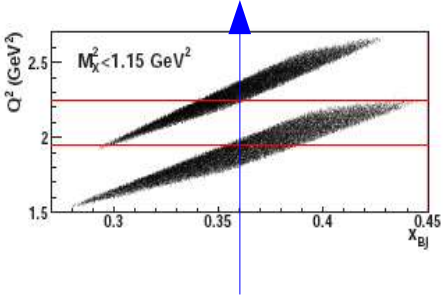

Results: Q^2 dependence

$(x_{Bj} = 0.36)$

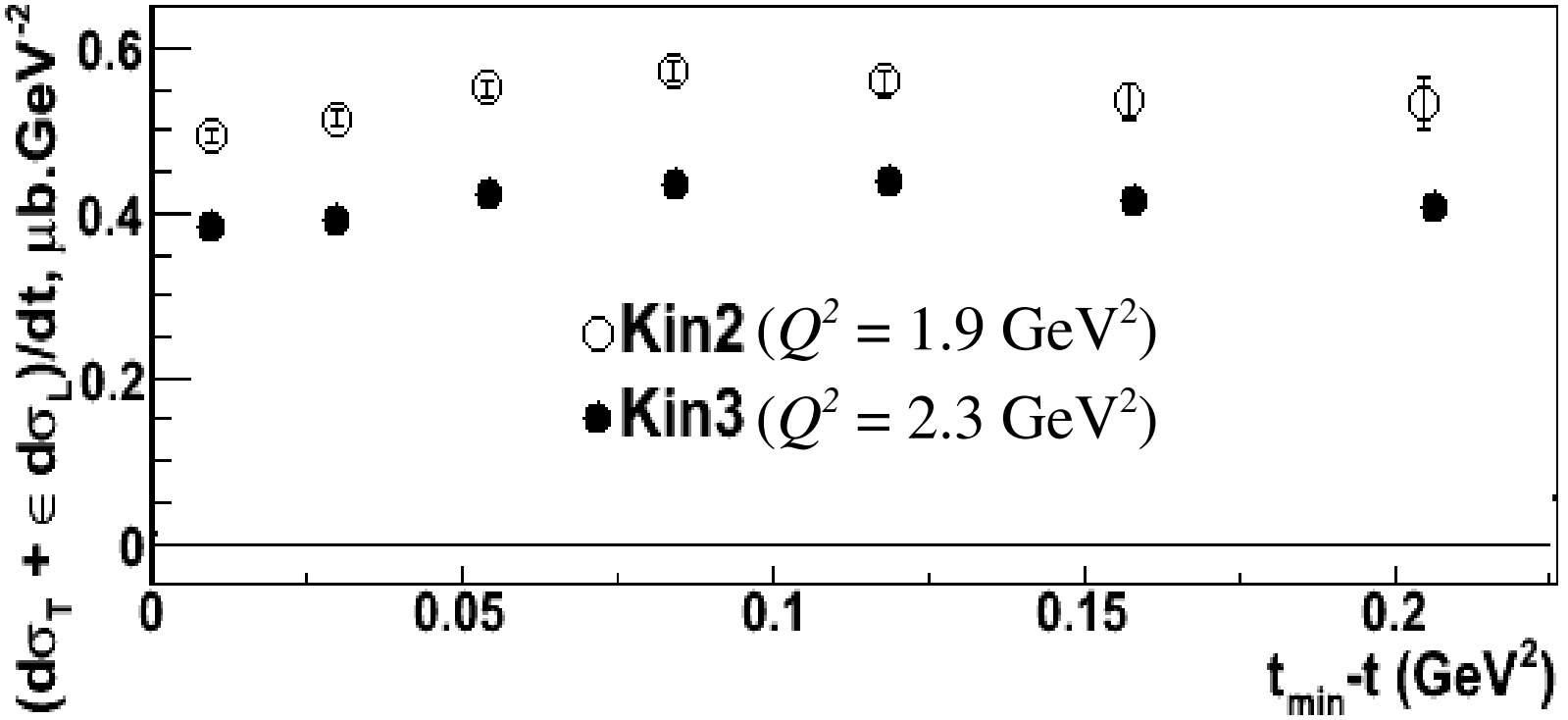

$\sigma_T + \epsilon_L \sigma_L$

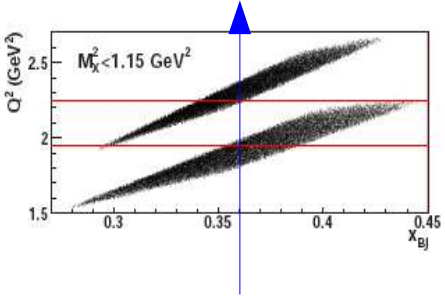

Results: Q^2 dependence

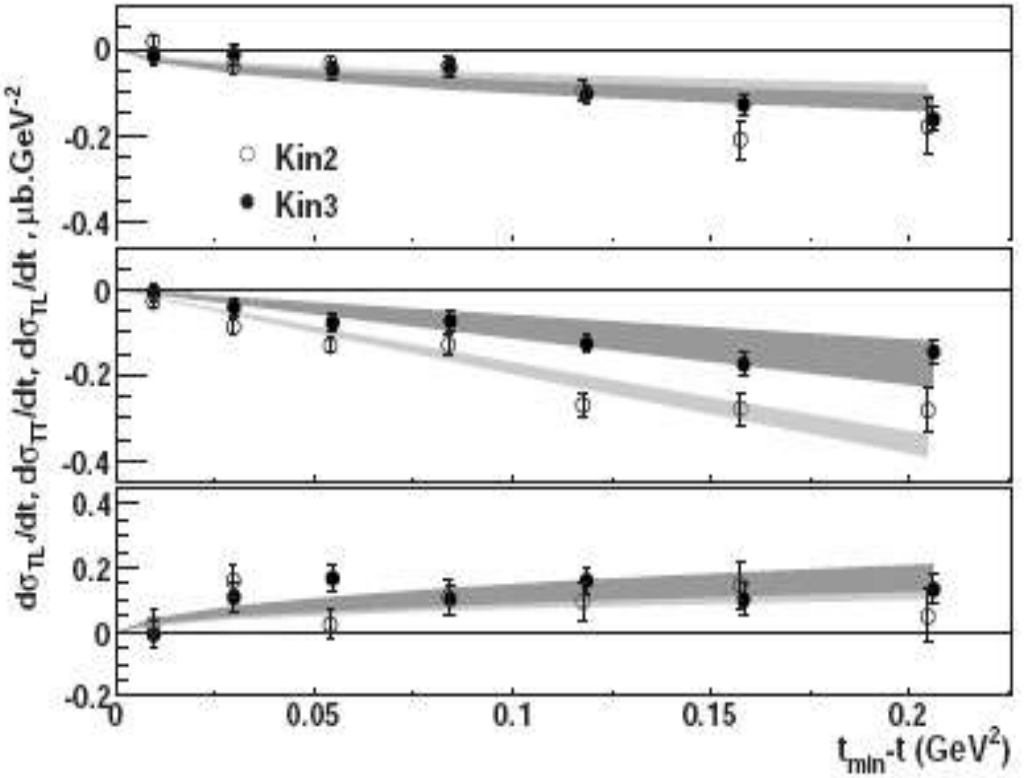

σ_{TL}

σ_{TT}

$\sigma_{TL'}$

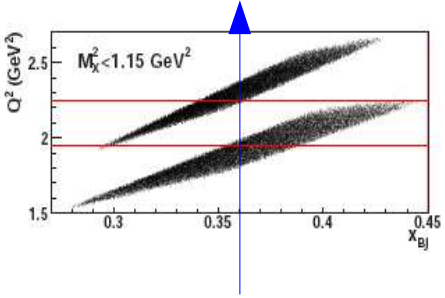

Results: Q^2 dependence

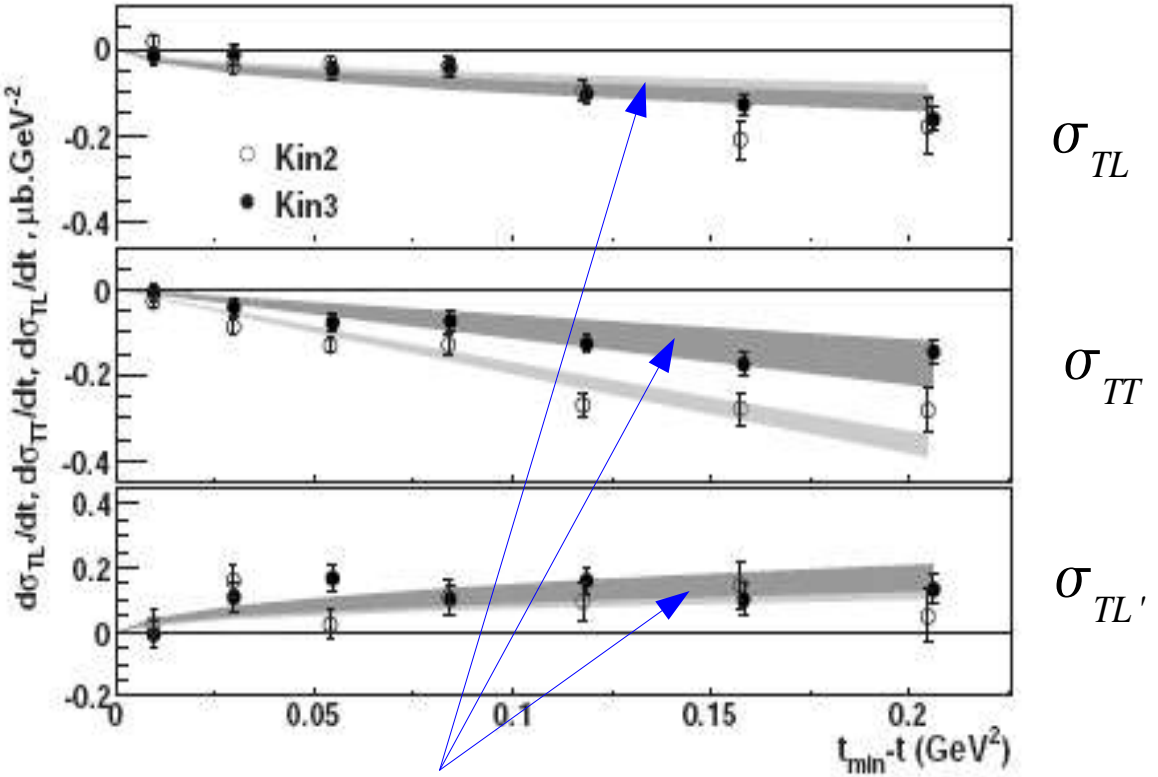

Fits $\propto \sin\theta_{\pi}^{CM}(\sigma_{TL}), \sin^2\theta_{\pi}^{CM}(\sigma_{TT}), \sin\theta_{\pi}^{CM}(\sigma_{TL'})$

=> leading geometrical dependences of the hadronic tensor

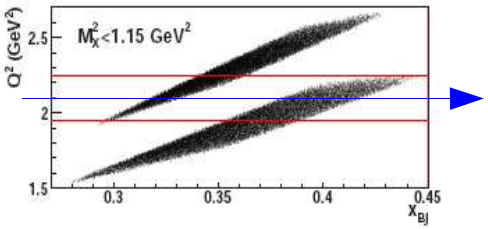

Results: *W* dependence

$(Q^2 = 2.1\ \mathrm{GeV}^2)$

$\sigma_T + \epsilon_L \sigma_L$

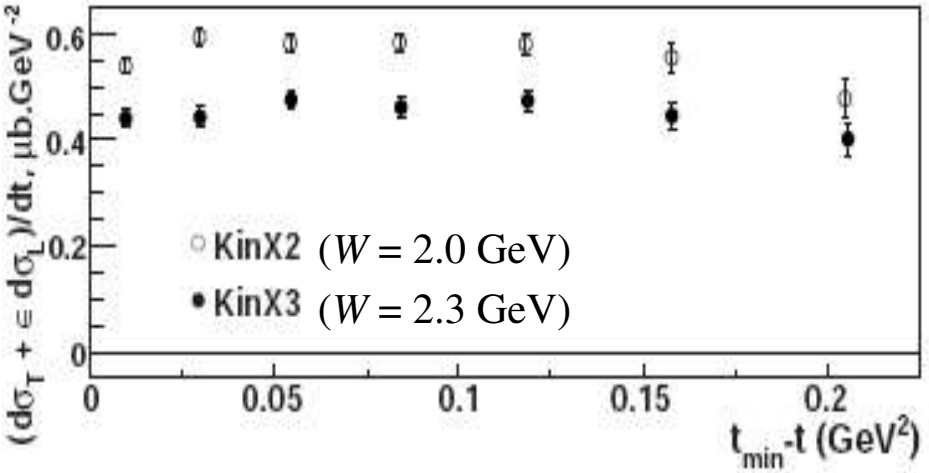

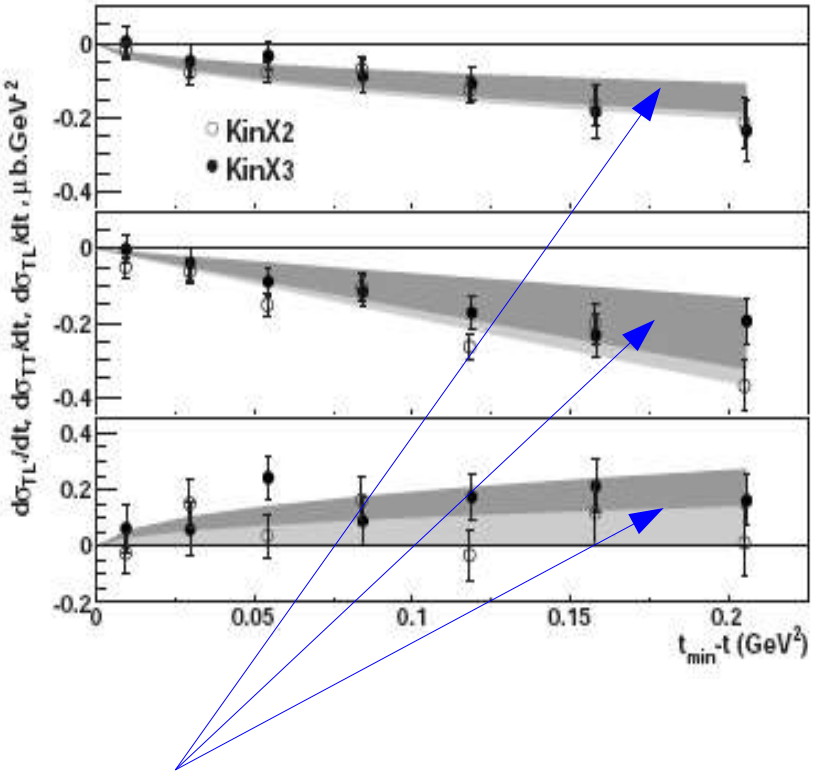

Fits $\propto \sin\theta_\pi^{CM}(\sigma_{TL}), \sin^2\theta_\pi^{CM}(\sigma_{TT}), \sin\theta_\pi^{CM}(\sigma_{TL'})$

Regge phenomenology inspired *t*-channel meson exchange model:
JM Laget [arXiv:**1004.1941**[hep-ph], talk of JM tuesday]:

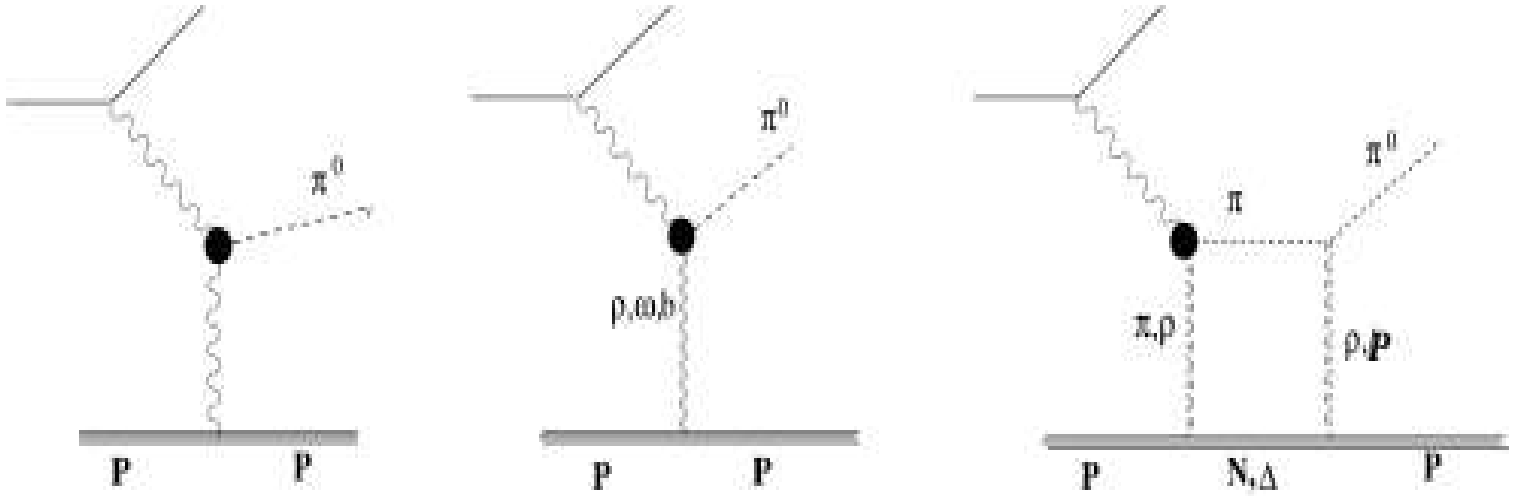

$+\rho^{+}\Delta^{0}$
$+\rho^{-}\Delta^{++}$

Primakoff **meson exchange** **meson exchange + Rescattering**

- Reproduces well photoproduction data, and low Q2 data at DESY.
- Reproduces Hall B π^0 BSA data [R. De Masi *et al.*, PR**C77**: 042201 (2008)] and Hall C π^+ longitudinal cross section [T. Horn et al., PR**C78**: 058201 (2008)]

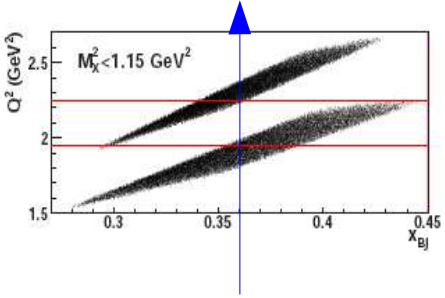

[arXiv:**1004.1941**[hep-ph]]:

Model curves:

solid: **total**

dashed: *partial contributions*

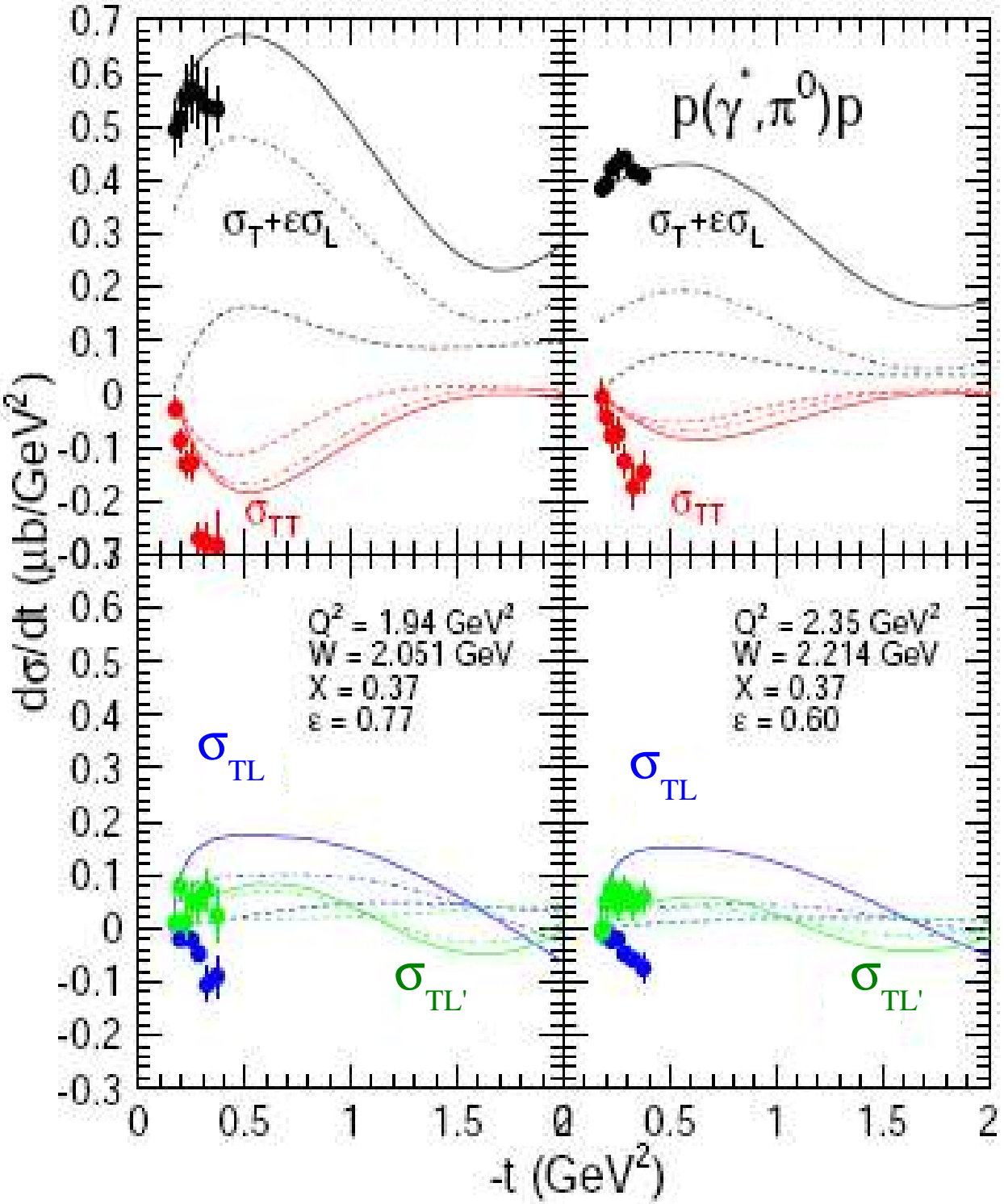

Regge and GPDs π^0 electro-production model by S. Liuti, G. Goldstein, S. Ahmad [PR**D79**, 054014 (2009)]

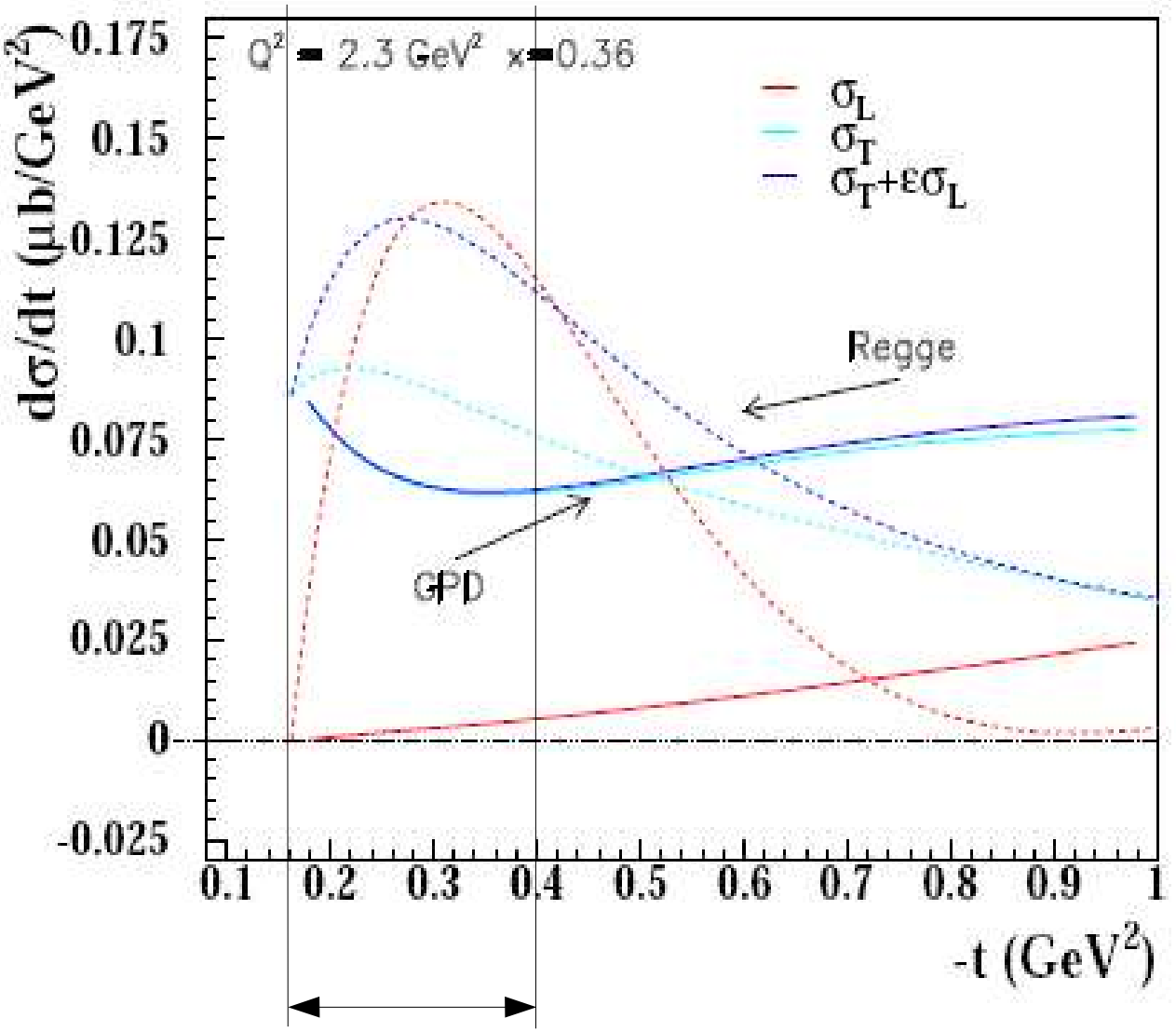

our data range

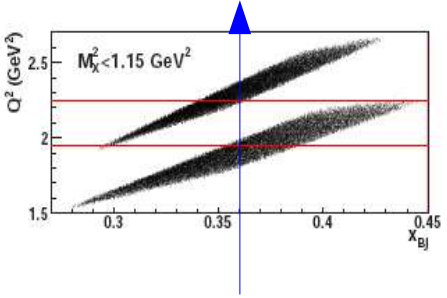

Q^2 dependence of hadronic tensor $(W_{xx}+W_{yy})/2+\varepsilon_L W_{zz}$

$$\frac{\left[(W_{xx}+W_{yy})/2+\epsilon_L W_{zz}\right]_{Kin2}}{\left[(W_{xx}+W_{yy})/2+\epsilon_L W_{zz}\right]_{Kin3}}=0.949\pm0.013\equiv\left(\frac{1.940}{2.353}\right)^{n}$$

Q^2 Kin2 (numerator) / Q^2 Kin3 (denominator)

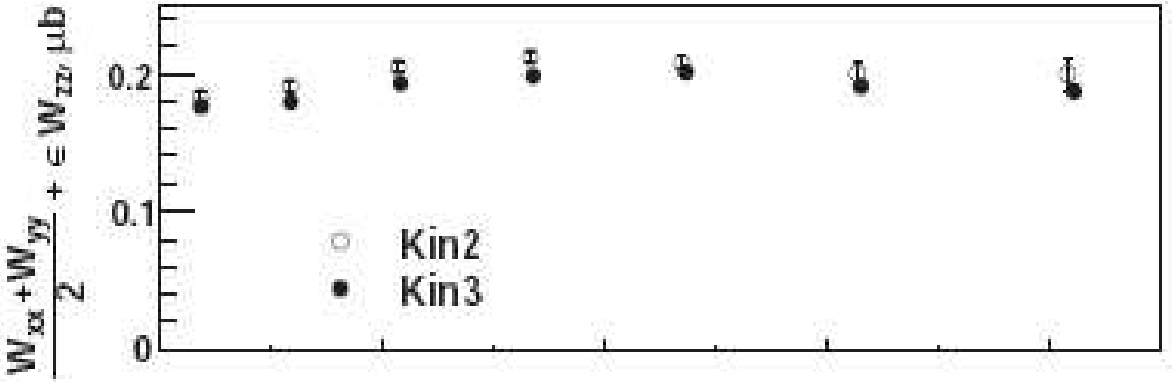

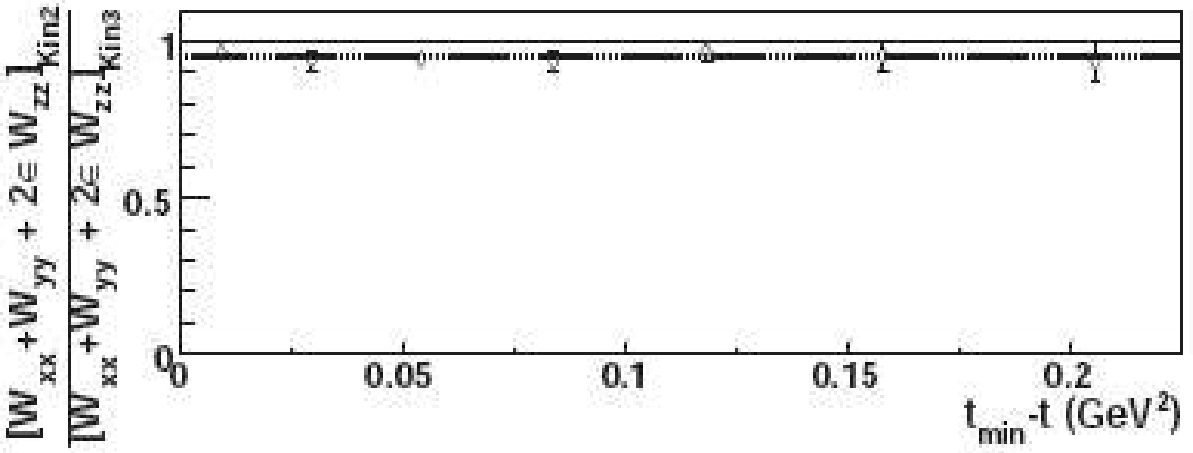

$$\frac{W_{xx}+W_{yy}}{2}+\epsilon_L W_{zz}\propto(Q^2)^{-0.27\pm0.07}$$

=> almost independent of Q^2

($\sigma_L^{VGG}\sim Q^{-0.48+/-0.11}$ if $\sigma_T \ll \sigma_L$)

-> too weak for $\sigma_L \sim Q^{-6}$ of GPDs...

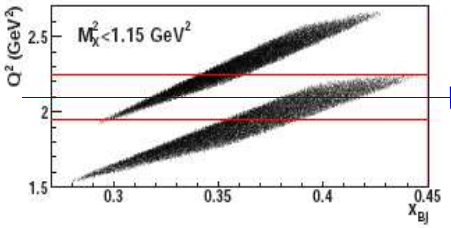

W dependence of hadronic tensor $(W_{xx}+W_{yy})/2+\varepsilon_L W_{zz}$

$$\frac{\left[(W_{xx}+W_{yy})/2+\epsilon_L W_{zz}\right]_{KinX2}}{\left[(W_{xx}+W_{yy})/2+\epsilon_L W_{zz}\right]_{KinX3}} = 1.004 \pm 0.021 \equiv \left(\frac{2.017}{2.272}\right)^n$$

W KinX2

W KinX3

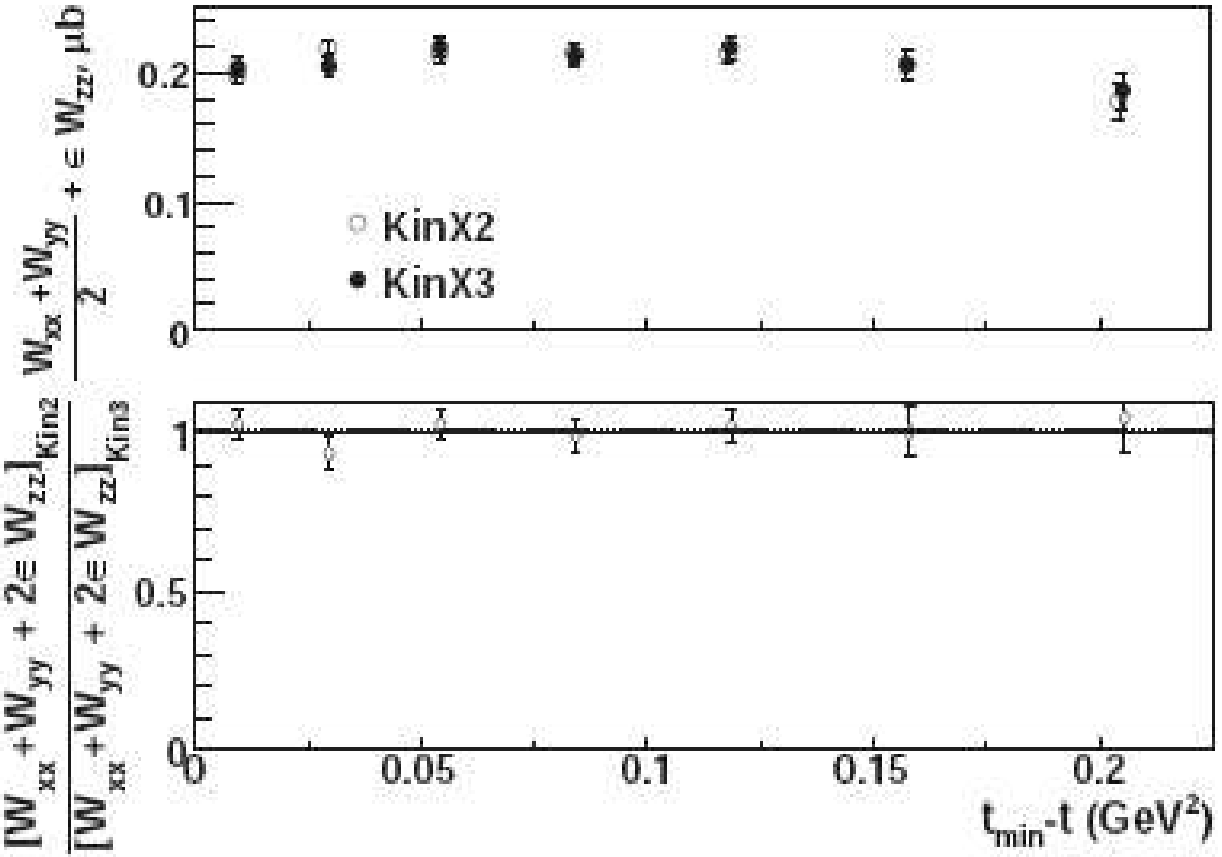

$$\frac{W_{xx}+W_{yy}}{2}+\epsilon_L W_{zz} \propto (W)^{0.03\pm0.18}$$

=> independent of *W*

What we learn from our data:

1) *t*-channel meson exchange model is able to describe $\sigma_T + \varepsilon_L \sigma_L$ and $\sigma_{TL'}$ but not σ_{TL} , σ_{TT}.

2) GPDs are not able to describe $\sigma_T + \varepsilon_L \sigma_L$

(Q^2-dependence too weak ≠ Q^{-6}). (σ_L alone ?)

What we learn from our data:

1) *t*-channel meson exchange model is able to describe $\sigma_T + \varepsilon_L \sigma_L$ and $\sigma_{TL'}$ but not σ_{TL} , σ_{TT}.

2) GPDs are not able to describe $\sigma_T + \varepsilon_L \sigma_L$

(Q^2-dependence too weak ≠ Q^{-6}). (σ_L alone ?)

=> This suggests:

1) far from QCD leading twist => σ_T dominant.

2) quasi flat Q^2-dependence => incoherent scattering on the quarks .

+ Work of Kaskulov *et al.* [Phys. Rev. **D78**: 114022, (2008)]

=> exclusive limit of SIDIS ?

π^+ cross sections published in Hall C: σ_L described by *t*-channel meson exchange model, but (without charged ρ channels) not σ_T.

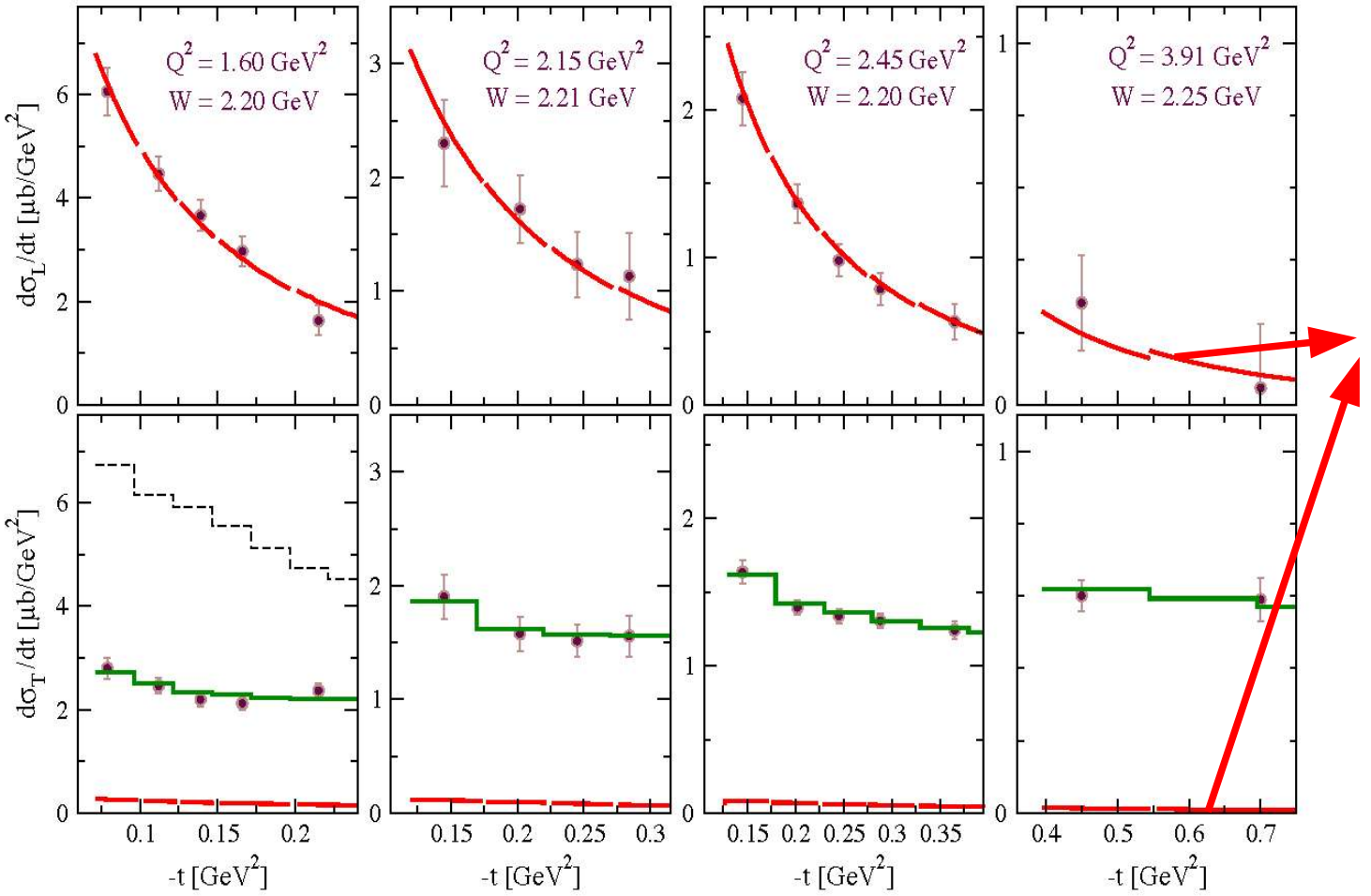

π^+ cross sections published in Hall C: σ_L described by *t*-channel meson exchange model, but (without charged ρ channels) not σ_T.

- M. Kaskulov *et al.* [Phys. Rev. **D78**: 114022, (2008)] performed calculations with PYTHIA-JETSET (Lund model), applied to Hall C π^+ transverse cross section.

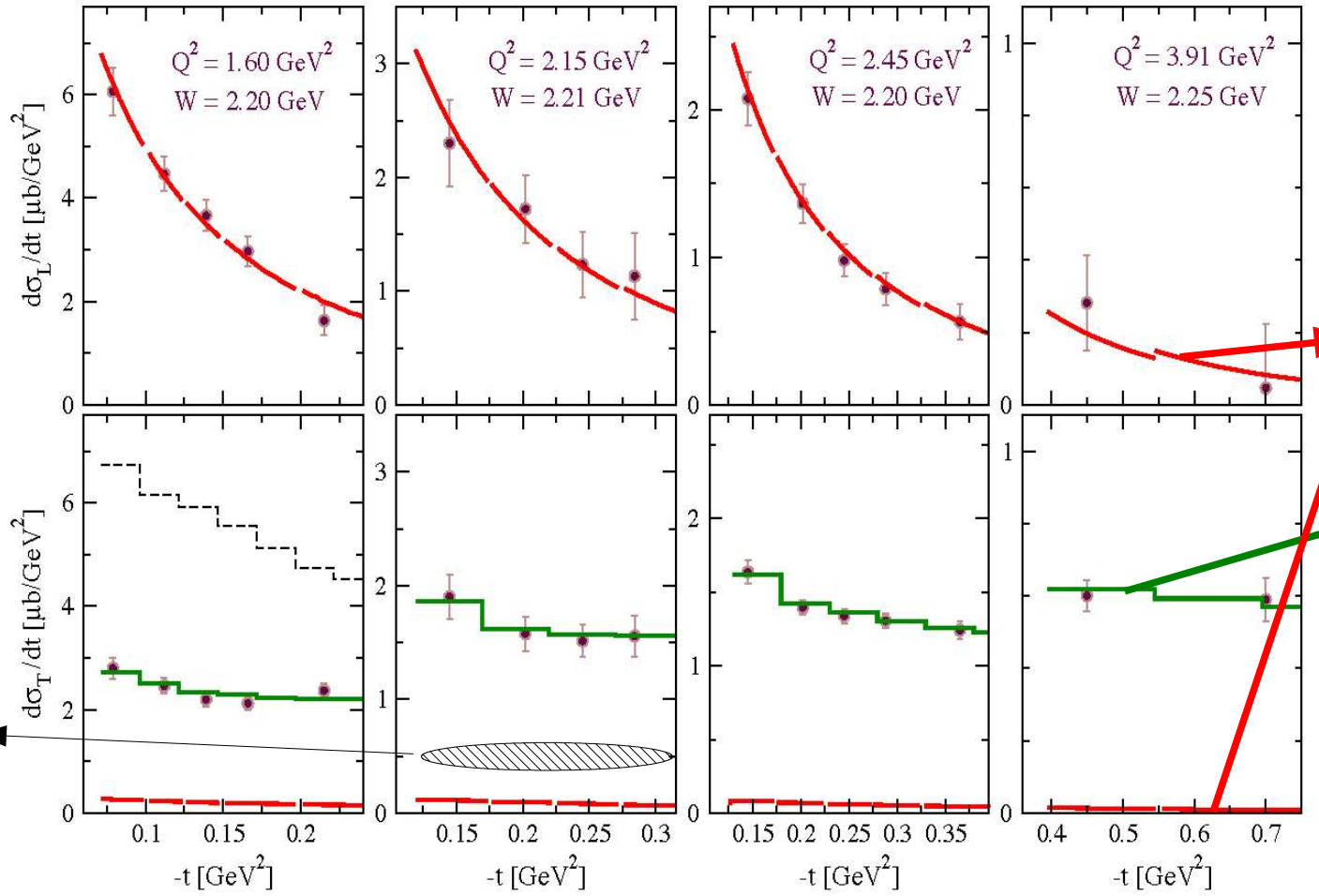

t-channel meson exchange model

Lund

Our π^0 data

Comparison of our data to a modelization of SIDIS by M. Anselmino *et al.* [Phys. Rev. **D71**: 074006, (2005)]

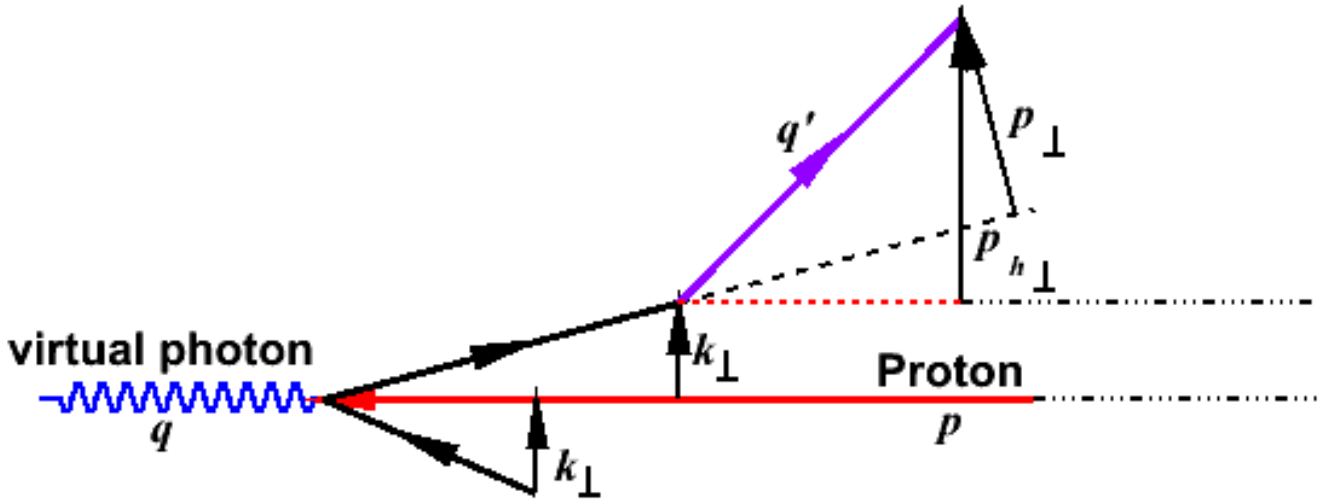

$$\frac{d^5\sigma^{\ell p\to \ell h X}}{dQ^2\, dx_{Bj}\, dz\, d^2 p_{h\perp}} \simeq \sum_q \frac{2\,\pi\alpha^2\, e_q^2}{Q^4} f_q(x_{Bj}) D_q^h(z)$$

$$\times\left[1+(1-y)^2 - 4\frac{(2-y)\sqrt{1-y}}{\frac{\langle p_\perp^2\rangle}{\langle k_\perp^2\rangle}(1+z^2)\sqrt{Q^2}}\, z\, p_{h\perp}\cos\phi_h\right] \times \frac{1}{\pi\langle p_{h\perp}^2\rangle} e^{-\frac{p_{h\perp}^2}{\langle p_{h\perp}^2\rangle}}$$

$$\equiv \sigma_T + \epsilon_L \sigma_L \qquad \equiv \sigma_{TL}$$

$$z = \frac{p\cdot q'}{p\cdot q}$$

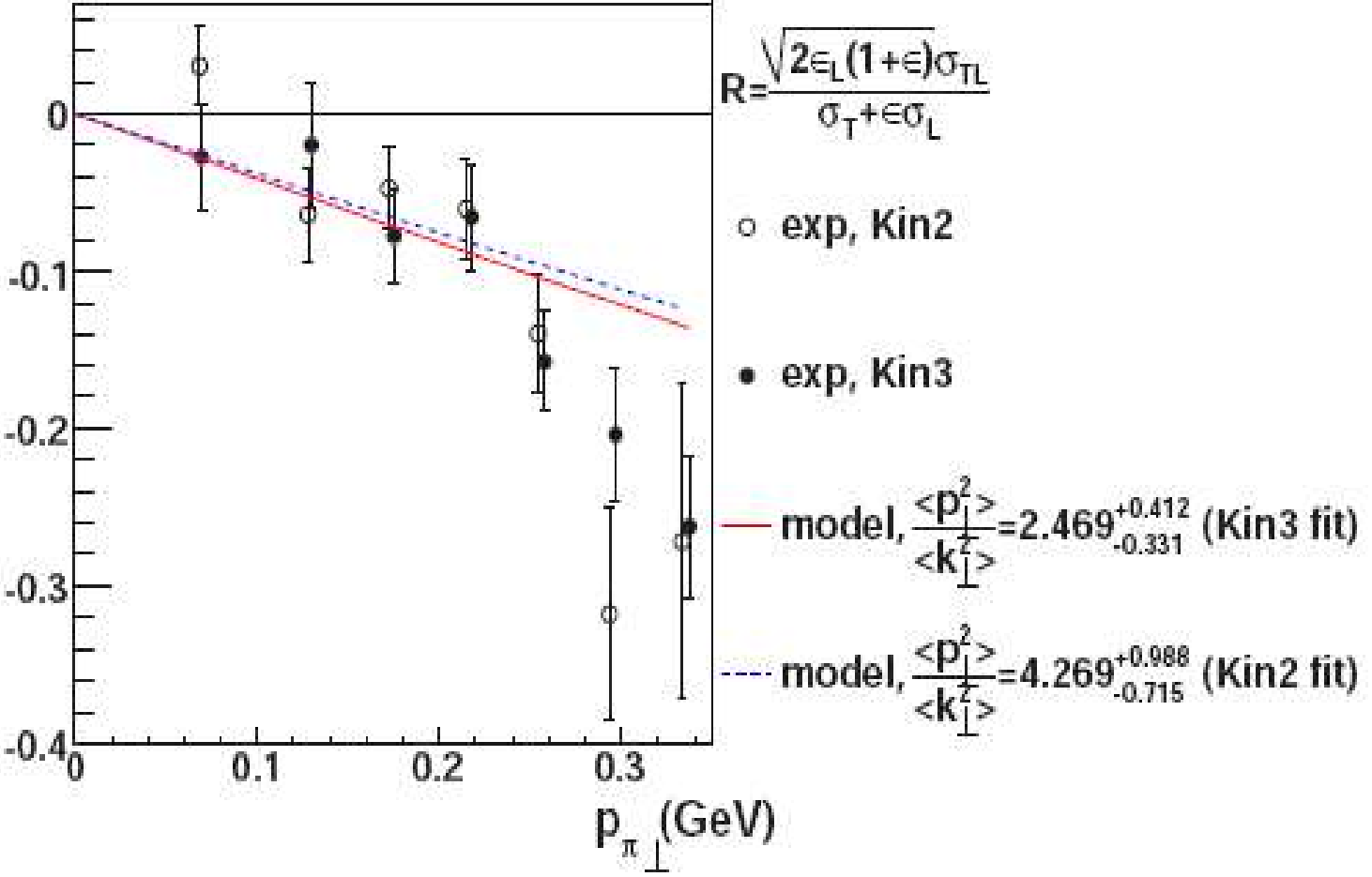

Agreement in sign and shape, if $\langle p_\perp^2 \rangle \simeq 3 \times \langle k_\perp^2 \rangle$

However, Anselmino extracted from SIDIS data: $\langle p_\perp^2 \rangle \simeq 0.8 \times \langle k_\perp^2 \rangle$

Our data: *z>0.9*, beyond limit of 2π, 3π production (multiplicity = 1).

SIDIS data (Anselmino analysis): multiplicity >> 1

Conclusions for Hall A π^0 experiment

We measured all separated ϕ contributions of the cross section. They indicate:

- t-channel meson exchange model able to describe $\sigma_T + \varepsilon_L \sigma_L$, but still needs improvement.
- Far from QCD leading twist behavior (σ_L alone ?).
- σ_{TL} sign consistent with the Cahn effect of SIDIS.

To improve understanding of our data, need transverse-longitudinal separation.

=> New DVCS/π^0 experiment in Hall A at the end of this year.

Back-up

Pion electro-production: Quantities of interest (in one photon exchange approximation)

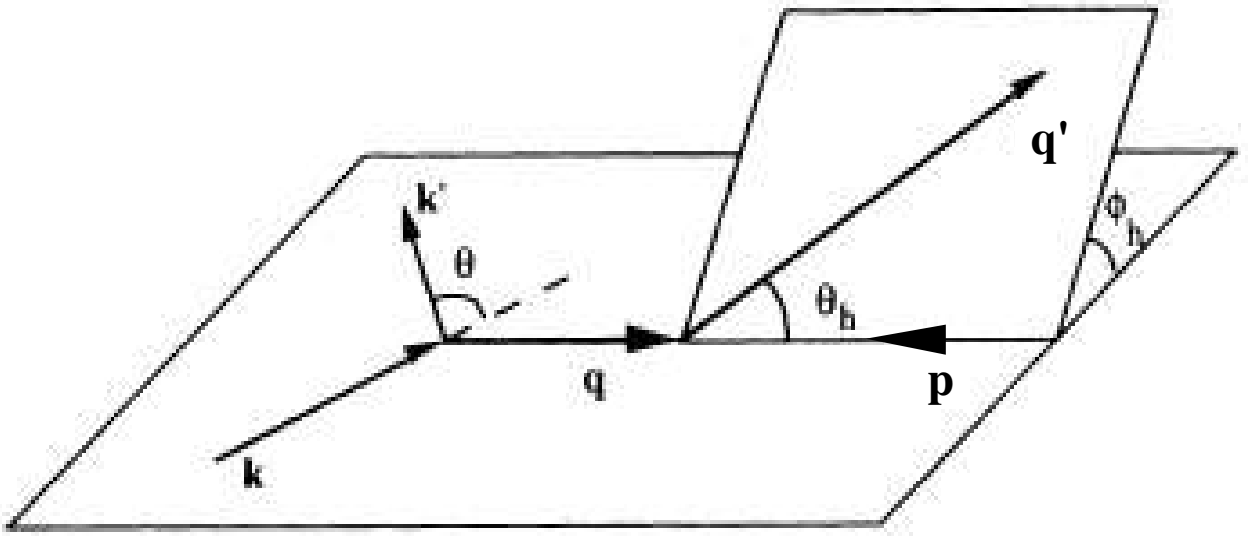

$$Q^2 = -q^2 = -(k - k')^2$$

$$W^2 = s = (q + p)^2 = M^2 + 2\,p.q - Q^2$$

$$t = (q - q')^2$$

$\Rightarrow t_{min}$ depends only on the electron.

$$\theta_\pi, \phi_\pi$$

NB: sometimes, x_{Bj} used instead of W.

Cross section analysis:

$$m_{\gamma\gamma}=\sqrt{(q_1+q_2)^2} \qquad M_X^2=(k+p-k'-q_1-q_2)^2$$

Because of calorimeter resolution, $\gamma\gamma$ invariant mass and missing mass squared are correlated.

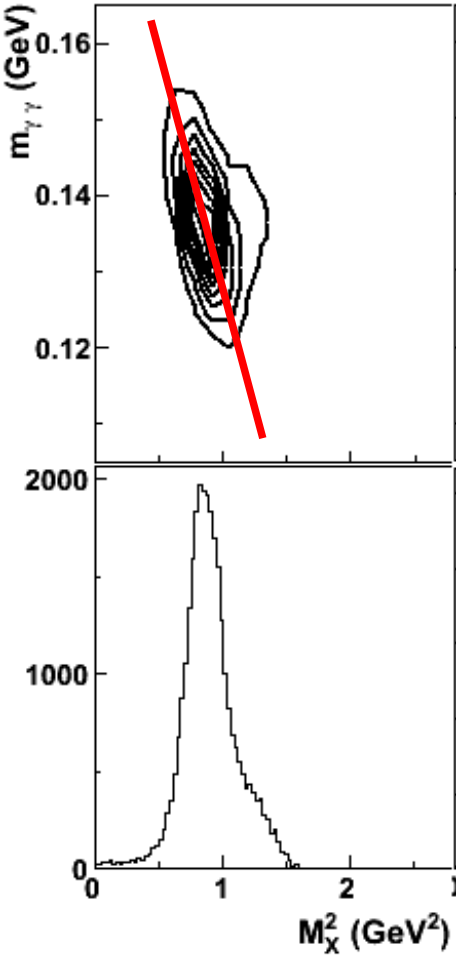

Cross section analysis:

$$m_{\gamma\gamma}=\sqrt{(q_1+q_2)^2} \qquad M_X^2=(k+p-k'-q_1-q_2)^2$$

Because of calorimeter resolution, $\gamma\gamma$ invariant mass and missing mass squared are correlated.

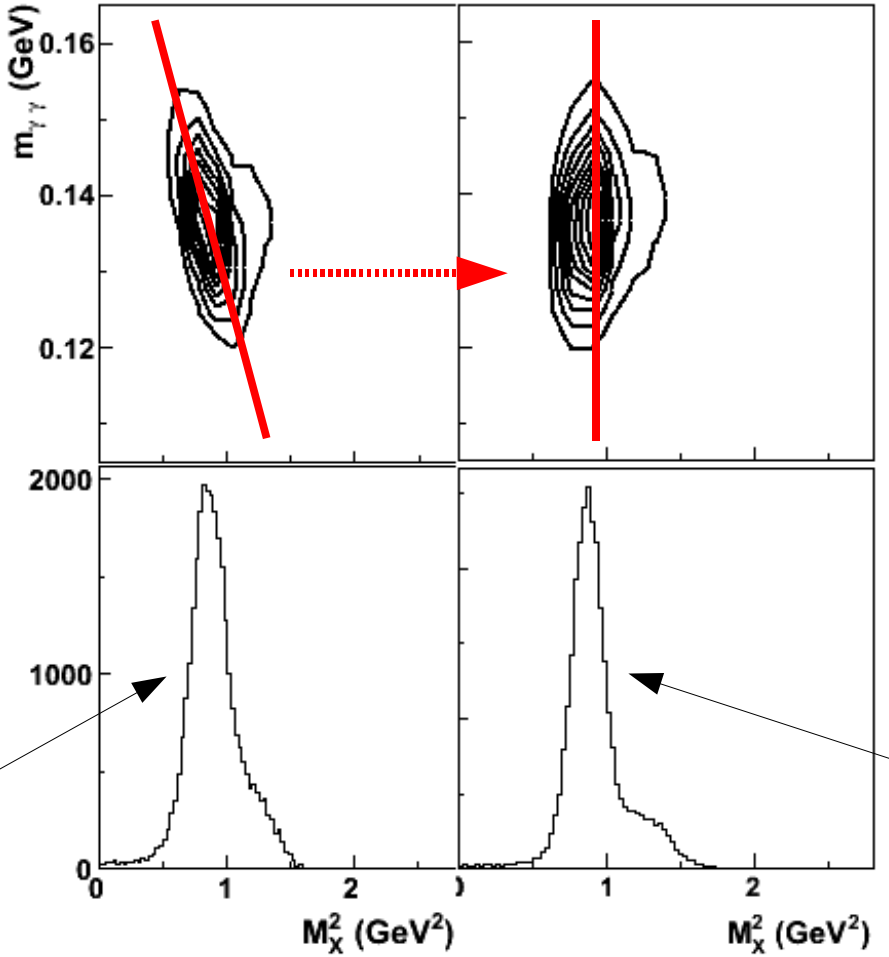

FWHM~ 0.34 GeV^2

FWHM~ 0.26 GeV^2

Calibration

Data calibration:

We know: $\Delta M_X^2 = \langle (M_X^2) \rangle - M_P^2 = 2\ \Delta q_\mu^i \left(E_X - \frac{\vec{P}_x \cdot \vec{q}_\mu}{|\vec{q}_\mu|} \right)$ → neglected

For all events, correct the two photon energies with: $\Delta q_\mu^i = \frac{\langle (M_X^2)_\mu \rangle - M_P^2}{2\ (E_X)^i}$

(The energy of each cluster is supposed to be given by the block μ collecting the largest fraction of the cluster energy)

Correction of the two photons brings correlations between the blocks calibration coefficients:
=> need several iterations to converge.

Simulation calibration:

Same principle as data calibration, except we smear the simulation resolution simultaneously, with a gaussian distribution.

At iteration n:

$$(q_\mu^i)_n = Gauss\left((q_\mu^i)_{n,mean}, \frac{\Delta\sigma_\mu}{\sqrt{2}}\right)$$

with $$(q_\mu^i)_{n,mean} = \left|q_\mu\right|_{n-1}^{i}\left(1 + \frac{\langle (M_X^2)_\mu \rangle_{simu} - \langle (M_X^2)_\mu \rangle_{data}}{4\ (E_X)^i}\right)$$

and $$\Delta\sigma_\mu = \sqrt{(\sigma_\mu)_{data}^2 - (\sigma_\mu)_{simu}^2}, \quad (\sigma_\mu)_{data} > (\sigma_\mu)_{simu}$$

$$\Delta\sigma_\mu = 0, \quad (\sigma_\mu)_{data} < (\sigma_\mu)_{simu}$$

Block Number	Data calibration coefficients		Simulation calibration/smearing coefficients			
	Kin2	Kin3	Kin2		Kin3	
0	0.0086845	0.0364559	0.180639	0.00527536	0.00550455	0.0262491
1	-0.00990708	-0.0742264	0.130999	0.00537773	0.0739439	0.0115104
2	-0.0726308	-0.0658277	0.0926654	0.00605774	0.0707933	0.00746904
3	-0.0333082	-0.166711	0.143432	0.00310192	0.0263115	0
4	0.0118644	-0.204987	0.151848	0.00922149	0.0584557	0.000423172
5	0.0232567	-0.0296373	0.0867122	0.0127546	0.0341923	0.0171308
6	-0.0772629	-0.199324	0.125425	0.00717858	0.00769925	0.0164821
7	-0.0551325	-0.0751047	0.164162	0.00907213	0.0357149	0.000891451
8	-0.0315943	-0.116005	0.148438	0.00653338	0.060819	0.00309728
9	0.00219844	-0.10276	0.112162	0.000971791	0.062555	0
10	-0.0393518	-0.0682206	0.144413	0.00475999	0.0321576	0.0071145
11	-0.0506004	-0.167808	0.150983	0.000521899	0.00624132	0.00913526
12	-0.0924164	-0.191489	0.160109	0.00581363	0.014166	0
13	-0.0136219	-0.126852	0.140755	0.00152294	0.0207511	0
14	-0.0476429	-0.0968454	0.114793	0.00251263	0.00830108	0.00608358
15	-0.0332962	-0.0743505	0.0608971	0.00747697	0.00686705	0.00370362
16	0.0186272	-0.0370882	0.0985969	0.0104825	0.0144606	0.0101382
17	-0.0495369	-0.0720492	0.15942	0.00253644	0.0148308	0.00462723
18	0.0704421	-0.0551577	0.153229	0.0119939	0.0391295	0
19	-0.00353016	0.0978609	0.174897	0.00869811	0.0293031	0.0318926
20	0.0221911	-0.0891911	0.132761	0.00345087	-0.00298083	0.00906114
21	-0.116276	-0.185007	0.141254	0.00776731	-0.000287712	0.0143864
22	-0.0271304	-0.156378	0.135035	0.00591424	0.0318078	0
23	-0.0298032	-0.0439254	0.125145	0.00700329	-0.00965089	0.00364076
24	0.0344403	-0.0312485	0.0940444	0.00630751	0.0406814	0.0101565
25	0.0357256	-0.0513582	0.108792	0.00556557	-0.0229523	0.00228948
26	-0.00653215	0.0170002	0.107431	0.0103348	-0.00947785	0.0244137
27	-0.0317248	-0.0849693	0.092749	0.00576689	-0.00639486	0.00652489
28	-0.0473825	-0.16756	0.107053	0.017067	-0.0201832	0
29	-0.0138601	-0.0508821	0.122518	0	0.0346743	0.00542758

Block Number	Data calibration coefficients		Simulation calibration/smearing coefficients			
	Kin2	Kin3	Kin2		Kin3	
30	0.123244	0.0814823	0.1216	0.00518817	-0.0539225	0.0189729
31	0.0728	0.108358	0.0771133	0.0418416	-0.00557148	0.0435922
32	-0.0621122	-0.124164	0.115054	0	0.00703299	0
33	-0.0623913	-0.123254	0.0702657	0.00392847	3.78489e-05	0.00278314
34	0.0943201	0.173564	0.0681999	0.0126694	0.0235344	0.0243018
35	0.0155664	0.0961346	0.0985822	0.00689743	0.000668168	0.0551944
36	0.0204595	0.00495492	0.055754	0.012554	-0.0647846	0.00810325
37	-0.0247905	-0.0860581	0.115994	0.0159602	-0.0241888	0
38	0.0208139	-0.054953	0.109938	0	-0.0186039	0
39	0.0365422	-0.062355	0.0864782	0.00874695	0.0155365	0.0183822
40	0.137129	0.18789	0.107279	0.0158812	0.013684	0.014996
41	0.0434142	-0.0318881	0.0787811	0.0208994	0.0647533	0.0162731
42	-0.016824	-0.0822051	0.104571	0.00772597	-0.0166177	0
43	-0.0215884	-0.0643274	0.113043	0.00250251	0.0114535	0
44	0.0940325	0.17869	0.0877945	0.0183785	0.0351586	0.0401128
45	0.0198378	0.162593	0.102038	0.00555548	0.0330782	0.0372498
46	0.0444158	0.115924	0.0935705	0.0143507	0.0507051	0.10133
47	0.0134339	0.0274669	0.0773137	0.00870756	-0.0340019	0.013907
48	-0.0499409	-0.150932	0.106692	0.00433739	-0.00077951	0.00142355
49	0.0485847	0.0080183	0.106996	0.00585024	0.0305864	0.00617311
50	0.0184302	-0.181746	0.119288	0.0211865	0.0152751	0.00807999
51	-0.0147517	-0.0834977	0.137732	0.00768604	0.0576783	0.00419525
52	0.0234731	0.0486023	0.116879	0.0146152	0.0341768	0.00320309
53	0.0354611	0.0992742	0.066353	0.00948989	0.0598453	0.0213818
54	0.0716051	0.0917418	0.111345	0.0191182	0.0051294	0.0525175
55	-0.00977696	-0.00721182	0.116705	0.012218	0.0448508	0.0451461
56	-0.00421609	0.0303139	0.0872153	0.0120677	0.0158795	0.0311627
57	0.00852822	0.162041	0.100995	0.0229612	0.024131	0.0148882
58	0.012656	-0.00574006	0.104407	0.0022772	0.0615108	0.0245628
59	0.0304994	-0.0239052	0.115357	0.00236782	0.0246767	0.00645669

Block Number	Data calibration coefficients		Simulation calibration/smearing coefficients			
	Kin2	Kin3	Kin2		Kin3	
60	0.0111014	0.146238	0.142004	0.0137879	0.0873722	0.0312713
61	0.0121214	-0.0134449	0.201765	0.012798	0.0519962	0.0107112
62	-0.0729513	-0.0175576	0.141769	0.0307567	0.03745	0.0339047
63	0.00754051	-0.0424134	0.121765	0.040711	-0.0100302	0.0058784
64	0.0624272	0.176483	0.115309	0.0199975	0.0078516	0.102933
65	0.00505601	0.00956212	0.104303	0.0238603	-0.0030567	0.0408596
66	0.0155223	0.206806	0.137378	0.0182963	0.0551064	0.0744226
67	-0.0597776	-0.115527	0.151565	0.0155301	0.0694677	0.00840219
68	-0.0874192	-0.342439	0.147692	0.0037929	0.0508745	0.0121106
69	0.021764	-0.0381151	0.157746	0.0296057	0.0963389	0.067461
70	0.0591689	0.110121	0.184053	0.00297851	0.0595174	0.0822289
71	0.0392662	0.145535	0.207612	0.0213075	0.151514	0.0235013
72	-0.0484536	0.124715	0.17213	0.0331145	0.139137	0.0329027
73	-0.0459503	0.165627	0.166892	0.0414966	-0.0574971	0.0396528
74	0.0669142	0.225375	0.106323	0.0236095	0.0327562	0.0374257
75	0.0183052	0.0276273	0.109683	0.0205563	0.0800042	0.0609578
76	0.0216399	0.162653	0.113917	0.0188966	0.0987673	0.0789419
77	-0.0111729	-0.249273	0.0945588	0.0219745	0.0620515	0.0246356
78	0.127303	0.276659	0.148203	0.0103492	0.162133	0.0824237
79	0.0240419	-0.367348	0.186433	0.024851	0.0677577	0.0102292
80	0.178732	0.424669	0.14912	0.0173934	0.0283945	0.0892107
81	-0.00865521	0.158135	0.148055	0.0271843	0.0426676	0.0606846
82	0.00716715	0.184516	0.155883	0.0295319	0.1583	0.0473582
83	0.0122464	0.194969	0.0749581	0.038438	0.0994545	0.147133
84	0.127051	0.532026	0.0794058	0.028957	-0.0579295	0.0545909
85	0.0506588	0.121267	0.160252	0.0460135	0.0222587	0.0560722
86	0.0612668	0.247675	0.157093	0.025088	-0.0293417	0.0737299
87	0.0633261	0.22261	0.132246	0.0183635	0.14226	0.0473525
88	0.179754	-0.170622	0.181867	0.031452	0.0539586	0.0214386
89	0.106486	0.0567889	0.159629	0.0268309	0.315621	0.205977

Extraction

$$\Delta N(j_d) = \mathcal{L}u \times \int_{\Delta x_d} dx_d \int_{\Delta x_v} dx_v \mathcal{R}(x_d, x_v) \otimes \sum_{\Lambda} \mathcal{F}_{\Lambda}(x_v) r_{\Lambda} = \sum_{j_v} K^{\Lambda}_{j_d, j_v} r_{\Lambda}$$

$$K^{\Lambda}_{j_d, j_v} = \mathcal{L}u \int_{\Delta x_d} \sum_{j_v} \int_{\Delta x_v} dx_d dx_v \mathcal{R}(x_d, x_v) \otimes \sum_{\Lambda} \mathcal{F}_{\Lambda}(x_v) = \mathcal{L}u \sum_{i \in \{j_v, j_d\}} \frac{\mathcal{F}_{\Lambda}(x_v)}{N_{Gen}} \Delta^5 \Phi$$

r_{Λ} extracted with a linear χ^2 method: $\chi^2 = \sum_{j_d} \frac{\left(\Delta N(j_d) - \sum_{j_v} K^{\Lambda}_{j_d, j_v} r_{j_v, \Lambda} \right)^2}{N_d}$

$$\Rightarrow \frac{d^5\sigma}{d^5\Phi} = \sum_{\Lambda} \mathcal{F}_{\Lambda}(\overline{x_{j_v}}) r_{\Lambda} \qquad \text{with : } \overline{x_{j_v}} = \frac{\sum_{i \in \Delta x_v} x_v K^{\Lambda}_{j_d, j_v} r_{j_v, \Lambda}}{\sum_{i \in \Delta x_v} K^{\Lambda}_{j_d, j_v} r_{j_v, \Lambda}} = \frac{\sum_{i \in \Delta x_v} x_v K^{T+\epsilon L}_{j_d, j_v}}{\sum_{i \in \Delta x_v} K^{T+\epsilon L}_{j_d, j_v}}$$

Pion electro-production formalism: coefficients for extraction

Remove all known kinematic dependences from the formalism bin per bin :

$$\frac{d\sigma_v}{d\Omega_\pi} = \frac{q'^{CM}}{k_\gamma^{CM}} \left(\frac{W_{xx}+W_{yy}}{2} + \epsilon_L W_{zz} + [2\,\epsilon_L(1+\epsilon)]^{1/2} \Re e\, W_{xz} + \epsilon \frac{W_{xx}-W_{yy}}{2} + h[2\,\epsilon_L(1-\epsilon)]^{1/2} \Im m\, W_{yz} \right)$$

$$r_T = \frac{W_{xx}+W_{yy}}{2} \qquad r_{TT} = \frac{1}{\sin^2\theta_\pi \cos 2\phi_\pi} \frac{W_{xx}-W_{yy}}{2} \qquad \begin{Bmatrix} r_{TL} \\ r_{TL'} \end{Bmatrix} = \frac{1}{\sin\theta_\pi} \begin{Bmatrix} -\frac{1}{\cos\phi_\pi} \Re e\, W_{xz} \\ \frac{1}{\sin\phi_\pi} \Im m\, W_{yz} \end{Bmatrix}$$

$$r_L = W_{zz}$$

$$\Rightarrow \frac{d^5\sigma}{d^5\Phi} = \sum_\Lambda \mathcal{F}_\Lambda(x_v) r_\Lambda \qquad (\Lambda \equiv [T+\epsilon L, TL, TT, TL'])$$

(r_Λ leading order in $\sin\theta_\pi^{CM}$ of CGLN amplitudes

[Chew, Goldberger, Low, Nambu, Phys. Rev. **106**, 1345 (1957)])

r_Λ extracted in all t_{min}-t bins by a linear fit (χ^2 method)

Cross section analysis

vertex $(Q^2, W, t_{min} - t, ...)_v \equiv x_v$ experimental $(Q^2, W, t_{min} - t, ...)_e \equiv x_e$

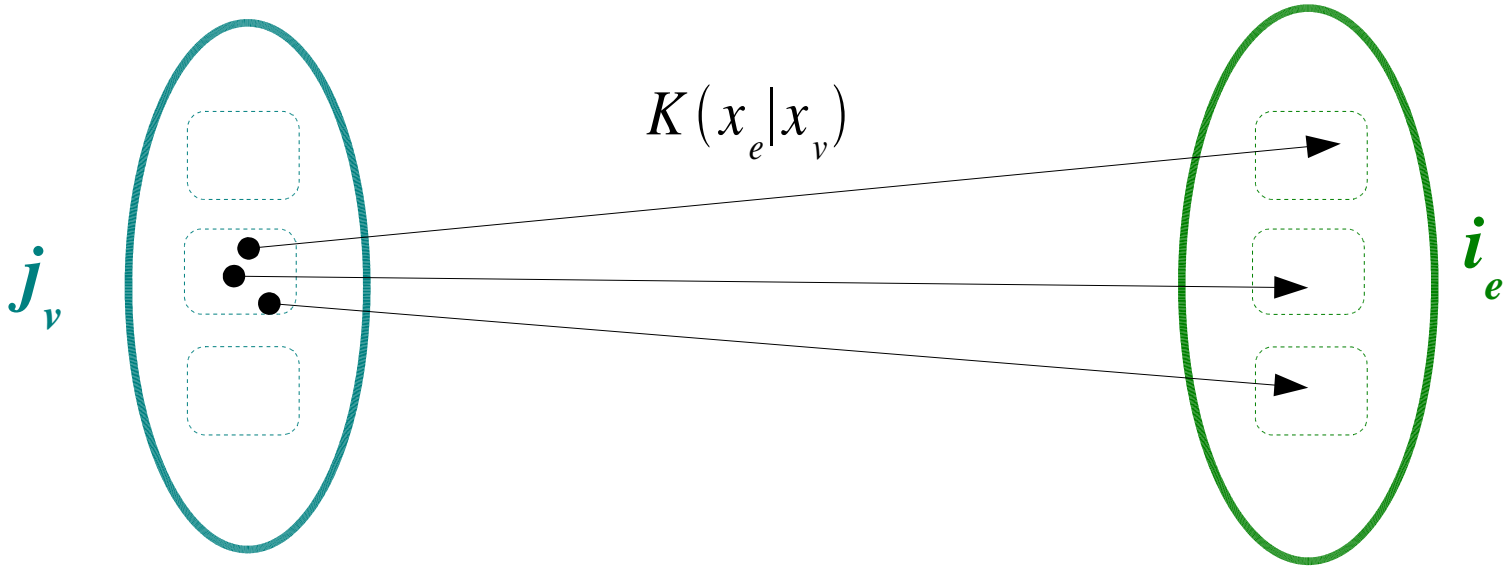

$$N(i_e) = \int_{x_e \in Bin\, i_e} dx_e \sum_{j_v} K(x_e|x_v) N(j_v)$$

due to detector resolution and efficiency, radiative effects...

=> Migrations of events from one bin to others.

Number of events in each bin proportional to set $\{r_\Lambda\}$

because of migrations we have to ignore the last t_{min}-t bin result.

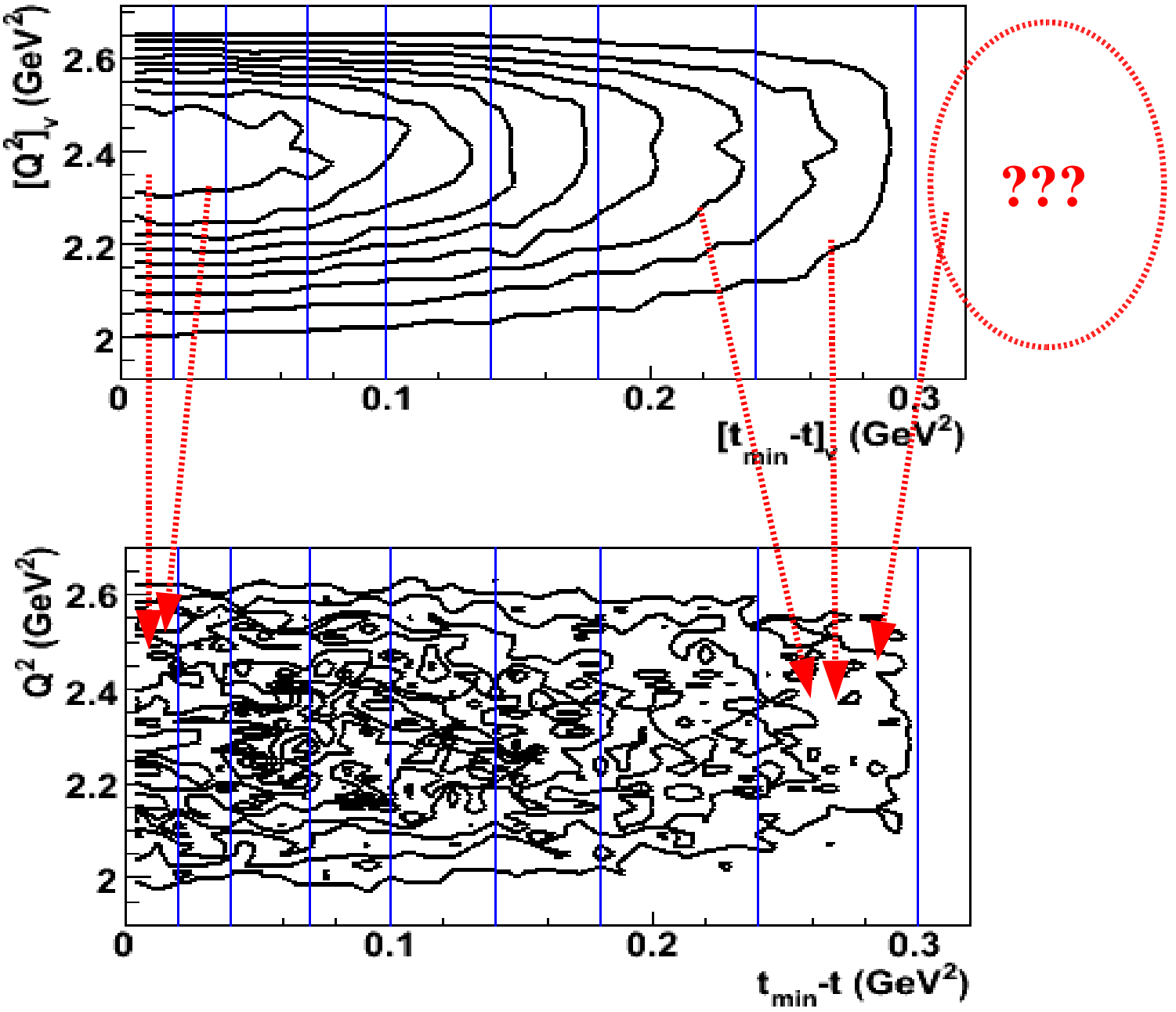

π^0 production contamination by $\omega \to \pi^0 \gamma$

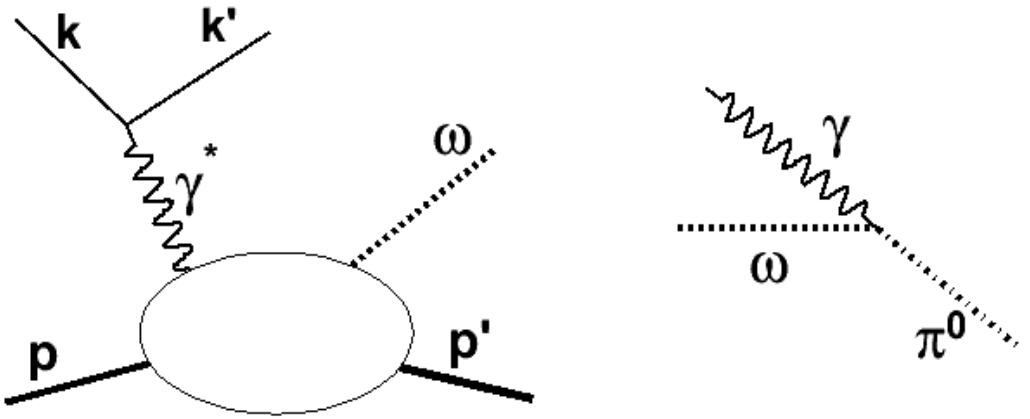

[L. Morand *et al.*, E.P.J **A24**, 445 (2005)]

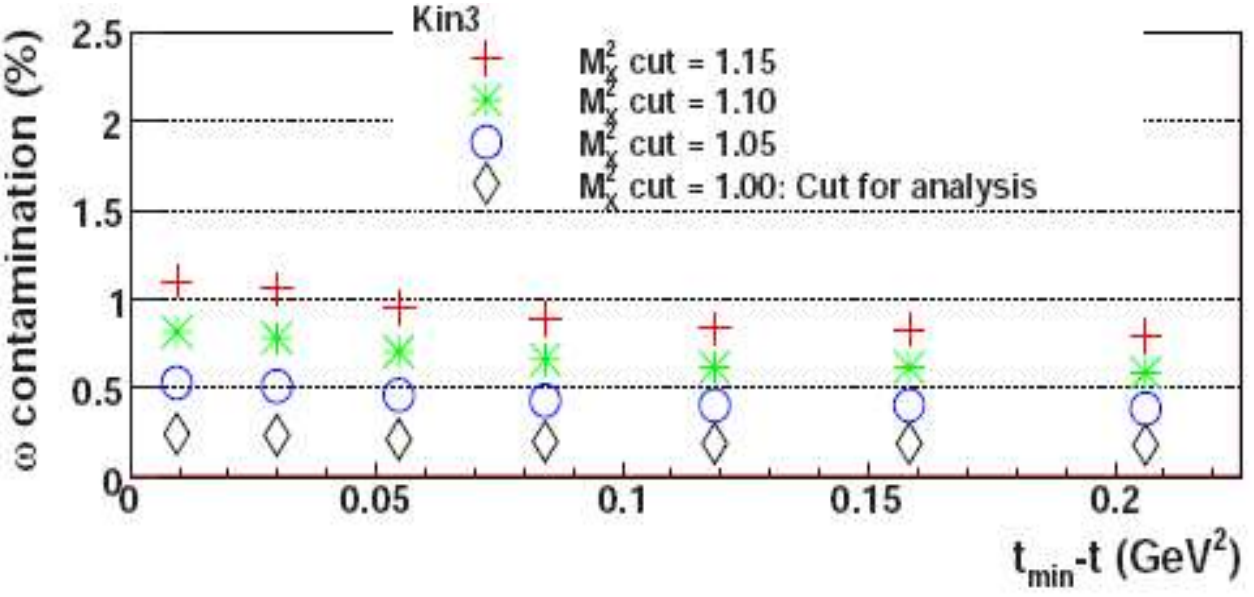

=> below 1% with our cuts

Calorimeter threshold:

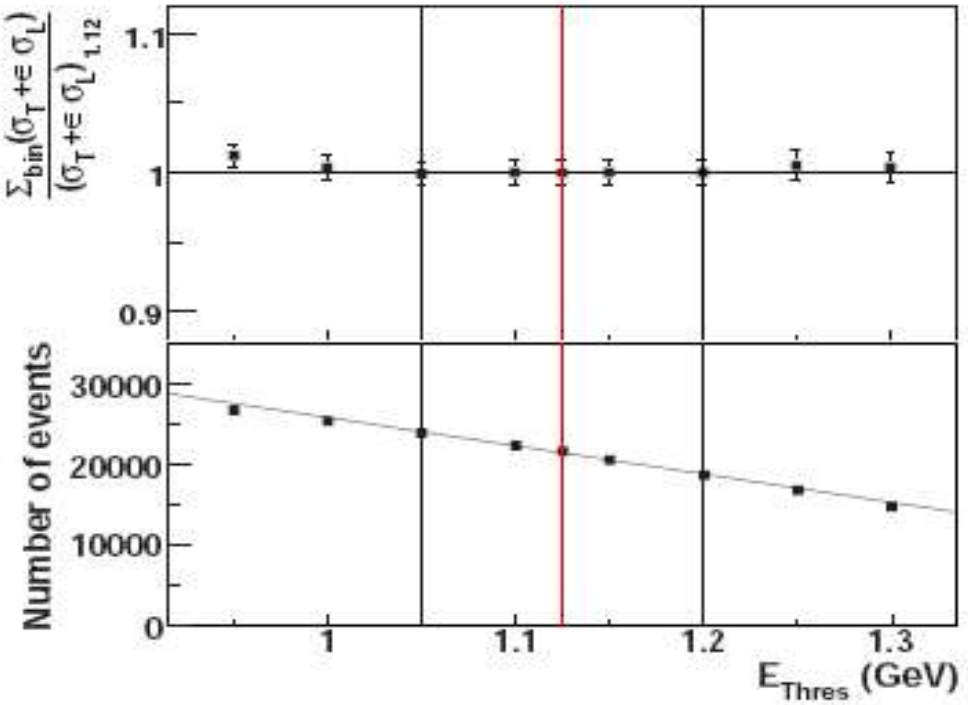

if E_{thr} too low -> hardware threshold: number of events is not relevant

if E_{thr} too high: removes too much statistics.